Summer 2023

Can Larvae of a Deep-Sea Gastropod, Thalassonerita naticoidea, Swim to the Surface to Find Food in the Gulf of Mexico?

Mitchell Hebner
Western Washington University, mg.hebner47@gmail.com

Can Larvae of a Deep-Sea Gastropod, *Thalassonerita naticoidea,* Swim to the Surface to Find Food in the Gulf of Mexico?

By

Mitchell Gregory Hebner

Accepted in Partial Completion
of the Requirements for the Degree
Master of Science

ADVISORY COMMITTEE

Dr. Shawn Arellano, Chair

Dr. Deborah Donovan

Dr. Brian Bingham

GRADUATE SCHOOL

David L. Patrick, Dean

Master's Thesis

In presenting this thesis in partial fulfillment of the requirements for a master's degree at Western Washington University, I grant to Western Washington University the non-exclusive royalty-free right to archive, reproduce, distribute, and display the thesis in any and all forms, including electronic format, via any digital library mechanisms maintained by WWU.

I represent and warrant this is my original work, and does not infringe or violate any rights of others. I warrant that I have obtained written permissions from the owner of any third party copyrighted material included in these files.

I acknowledge that I retain ownership rights to the copyright of this work, including but not limited to the right to use all or part of this work in future works, such as articles or books.

Library users are granted permission for individual, research and non-commercial reproduction of this work for educational purposes only. Any further digital posting of this document requires specific permission from the author.

Any copying or publication of this thesis for commercial purposes, or for financial gain, is not allowed without my written permission.

Mitchell Gregory Hebner

7/12/2023

Can Larvae of a Deep-Sea Gastropod, *Thalassonerita naticoidea,* Swim to the Surface to Find Food in the Gulf of Mexico?

A Thesis
Presented to
The Faculty of
Western Washington University

In Partial Fulfillment
Of the Requirements for the Degree
Master of Science

by
Mitchell Gregory Hebner
July 2023

Abstract

For benthic organisms that live in the deep-sea, the location from where their larvae begin their dispersal has a substantial influence on their vector of travel due to the different ocean current velocities the larvae could encounter, because ocean currents affect larval dispersal when the larvae are in the water column like during a possible vertical migration from the bottom water. The deep-sea is food-poor when compared to the relatively food-rich surface waters, but planktotrophic (feeding) larval development of deep-sea benthic organisms is common, especially in gastropods. Despite the potential need for planktotrophic larvae of deep-sea organisms to access more nutrient-rich food sources and knowing that a larva's position in the water column can impact larval transport, we have very little understanding of where in the water column the larvae of deep-sea organisms develop. To overcome challenges, in this work I used *Thalassonerita naticoidea,* formerly *Bathynerita naticoidea,* to study deep-sea larval migration potential by modeling the expended energy of *T. naticoidea* larvae while vertically swimming. The purpose of this study was to first examine how the swimming rates and metabolism of *T. naticoidea* larvae are influenced by water temperature. The energetics model of Young et al. (1996) was used to determine how much energy the larvae would expend while swimming vertically, and how much time these larvae would need to swim to the photic zone above the Brine Pool NR1 in the Gulf of Mexico. The model predicted that an average larva swimming vertically from a depth of 650.8 meters to 87.7 meters at a constant mean minimum velocity of 0.66 ± 0.04 m h^{-1} expend 111.7 mJ in 28.6 days to reach the photic zone (200 meters). A larva swimming vertically through the same depth range at a constant mean velocity of 1.43 ± 0.06 m h^{-1} will expend 52.7 mJ in 13.5 days to reach the photic zone. Finally, a larva swimming vertically at a constant mean maximum velocity of 2.22 ± 0.09 m h^{-1} will expend 31.6 mJ in 7.7 days to reach the photic zone. As the larvae vertically migrate from 650 meters up to the surface, they have access to food like dissolved organic materials and bacteria. Although, whether the larvae can assimilate dissolved organic materials without eating remains to be verified. Once at the surface, depending on the time of year, they have access to phytoplankton which they can eat to continue their development. Moreover, migration through a 650-meter water column will expose larvae to a dynamic current system that can ultimately impact their dispersal and population connectivity. In the future, vertical migration models, like the one derived in this study or from Young et al. (1996), can be incorporated with larval transport models to predict larval dispersal distances and population connectivity more accurately.

Acknowledgements

I would first like to thank my advisor Shawn Arellano for her unwavering mentorship, steadfast support, and contagious drive to always do better which has pushed me to be the scientist and person that I am today. I would also like to thank my esteemed committee members Deb Donovan and Brian Bingham for their great advice and friendly help, and for teaching me about physiological ecology and statistics. In addition, I am eternally grateful to Shawn and Craig Young for providing me with the cruise experiences that I am fortunate to be a part of.

I would like to express my sincere gratitude to the unyielding love and support of my parents. To my mother, who inspired me to become a biologist so very long ago, and here I am Ma, pursuing my dreams with your love and support. To my father, who helped me with some of the math in this thesis, in addition to providing love, guidance, support, and resources so I could devote my time to pursuing my dreams. Thank you both very much.

To my brother Evan, I am so proud to have you as a brother, and so inspired by your impeccable taste for the finer things in life. Whenever we get to spend time together, I am reminded of how much joy and laughter you bring to my life. To my brother Ethan, myself and a lot of people miss you every day. You would have loved to be a part of this journey and thanks for all the help and support from the other side.

To my partner Nina, thank you for standing by my side and helping me deal with the stresses of grad school, moving across the country, and for being the reason I smile most days in my life.

I would also like to thank my friends and family across the country who have made me feel proud for leaving home to accomplish my dreams. I miss you all, much love; *ad superficiem per aquam*.

Thank you to the friends that I have met along the way, including but not limited to: Dexter Davis, Tessa Beaver, Ahna Van Gaest, Michelle McCartha, Tanika Ladd, Vanessa Jimenez, Wyatt Heimbichner Goebel, Caitlin Plowman, Lauren Rice, Avery Calhoun, and all my fellow Bio 101 TA's at Western.

I wish to thank the Captain and Crew of the R/V *Atlantis* and the R/V *Thomas G. Thompson* for their efforts and help on the cruises that made my work and deep-sea experiences possible. Also, thanks to the crew of ROV Jason for collecting my samples in June 2021.

The work in this thesis is supported by an NSF grant to Shawn Arellano, the Ross and Flora Fellowship through the Biology department of Western Washington University, and from Washington State Sea Grant Dean John A. Knauss Marine Policy Fellowship.

Table of Contents

List of Figures

List of Tables

Can Larvae of a Deep-Sea Gastropod, *Thalassonerita naticoidea,* Swim to the Surface to Find Food in the Gulf of Mexico?

Introduction

For benthic organisms that live in the deep-sea, the location from where their larvae begin their dispersal has a substantial influence on their vector of travel (Fiksen et al., 2007; Young et al., 2012; McVeigh et al., 2017; Gary et al., 2020) due to the different ocean current velocities that larvae could encounter (Shanmugam, 2012), because ocean currents affect larval dispersal when the larvae are in the water column, for example, during a possible vertical migration from the bottom water. The deep-sea benthic boundary layer, the layer of water that exists above the sediment of the deep-sea can be several meters thick (Cartes, 1998), and is the combination of abiotic (*e.g.*, sinking of particles from the surface, turbulent mixing, and bottom currents) and biotic factors (*e.g.*, benthic organisms living, feeding, and reproducing) (Gili et al., 2020). In addition, the benthic boundary layer is slow-moving due to friction between the water and the sediment (Gili et al., 2020) which can limit the dispersal potential of larvae (Young, 1994). Whereas ocean currents in the mid-water and near the surface have relatively greater velocity and are the result of tides, the wind, and density differences due to temperature and salinity (NOAA, 2023). Therefore, whether the larvae of benthic deep-sea invertebrates migrate vertically and get transported by ocean currents above the deep-sea benthic boundary layer, or remain near the bottom water, can influence population dynamics of deep-sea ecosystems by impacting larval transport (Young et al., 2012; Teixeira et al., 2013; Gary et al., 2020).

The deep-sea is food-poor when compared to the relatively food-rich surface waters (Smith et al., 2008), but planktotrophic (or feeding) larval development of deep-sea benthic

organisms is quite common, especially in gastropods (Young et al., 2018). In the North Atlantic, gastropod species with planktotrophic larvae are more common on the abyssal plane than on the continental shelf (Young et al., 2018), meaning the larvae on the abyssal plane must migrate a greater distance to the surface than larvae migrating from the continental shelf. Additionally, three of the 30 gastropod species described in a study of the East Pacific Rise hydrothermal vent (~2500 m deep) have planktotrophic larvae (Young et al., 2018). Planktotrophic larvae do not have a yolk and need to feed to sustain their development (Nielsen, 2018), posing a challenge to larvae in a food-poor, deep-sea environment. H.N. Moseley, a naturalist on the *Challenger* expedition, first hypothesized in 1880 that larvae of deep-sea organisms may migrate into more food-rich surface waters to feed and develop (Young et al., 2018). Vertical migration of deep-sea planktotrophic larvae would offer increased exposure to food-rich waters. During a vertical migration from the deep, a larva could also be exposed to a variety of potential food resources such as bacteria and phytodetritus, phytoplankton in the surface waters, and dissolved organic matter (Boidron-Métarion, 1995). For deep-sea planktotrophic larvae that vertically migrate to access more nutrient-rich food, a potentially long vertical migration would influence the length of time they spend in the plankton, and providing deep-sea planktotrophic larvae the potential to disperse by exposing them to currents above the benthic boundary layer (Young et al., 2018).

Despite the potential need for planktotrophic larvae of deep-sea organisms to access more nutrient-rich food sources and knowing that a larva's vertical position in the water column can vastly impact transport, we have very little understanding of where in the water column the larvae of deep-sea organisms develop (Young et al., 2018). Larvae are relatively small when compared to the size and depth of the ocean, and searching for the larvae of deep-sea organisms is equivalent to searching for a needle in a sea of haystacks, thus, making it difficult to directly

assess their vertical distribution. Direct methods like surface plankton tows have yielded limited numbers of larvae from deep-sea species (Arellano et al., 2014; Bouchet & Warén, 1994). Instead, indirect methods to investigate larval migration have been used. For example, the analysis of carbon and oxygen isotopes present in the larval shells can indicate if deep-sea species develop near the relatively warmer surface waters but is only applicable to larvae with shells (Killingley & Rex, 1985; Bouchet & Warén, 1994). A second indirect method is the use of anatomical evidence. For example, the presence of light-sensitive eyes on larvae when there is no natural light in the deep-sea can be used to infer migration into more food-rich surface waters but does not provide a direct link to location or migration patterns (Bouchet & Warén, 1994). Our understanding is further limited because larvae are difficult to identify morphologically, and genetic analyses rely on reference libraries that currently include a small fraction of deep-sea fauna, making identification a challenge.

To overcome these challenges, I used *Thalassonerita naticoidea,* formerly *Bathynerita naticoidea* (Clarke, 1989), to study if a deep-sea larva has the potential for a vertical migration, I modeled the expended energy of *T. naticoidea* larvae while vertically swimming. *T. naticoidea* is a gastropod that lives on the shells of chemosynthetic mussels in cold-seep ecosystems of the Gulf of Mexico and the Caribbean. A small number of *T. naticoidea* veligers have been found in surface plankton tows above cold-seep sites that are 650 meters below in the Gulf of Mexico (Arellano et al., 2014). *T. naticoidea* is abundant and can be cultured and kept in a laboratory environment (Van Gaest, 2006). Previous data from this organism have shown that the larvae will eat algae, can have a larval lifespan of greater than 90 days when reared in the laboratory, and can swim for 16 days without food in the lab (Van Gaest, 2006). This gastropod is not believed to host chemosynthetic bacteria like many foundational cold-seep organisms do.

Instead, adults graze on bacteria and biofilm on the shells of *Gigantidas childressi* (Zande & Carney, 2001) and reproduce seasonally by depositing egg capsules on the mussel shells (Van Gaest, 2006). Fertilized oocytes are laid in egg capsules, typically between October and March with the greatest density deposited between December and February, and contain 25 to 180 embryos (Van Gaest, 2006). The embryos develop within the egg capsule for approximately four months (at 8°C), bypassing the trochophore stage, and hatch as swimming, feeding veligers between January and June (Van Gaest, 2006). The shell lengths have been sampled as larvae at the Brine Pool in February 2003, as larvae in the water column in 2003, and finally as juveniles at the Brine Pool in February 2004 (Van Gaest, 2006). The shell length increased during the three sampling events (Van Gaest, 2006). Combining their seasonal reproduction with the shell growth in a year allows us to estimate that *T. naticoidea* larvae have a planktonic larval duration ranging from 8-12 months (Van Gaest, 2006).

The purpose of my study was to first examine how the swimming rates and metabolism of *T. naticoidea* larvae are influenced by water temperature. The energetics model of Young et al. (1996) was then used to determine how much energy the larvae would expend while swimming vertically and how much time these larvae would need to swim to reach the photic zone. Combining experimental data and the model output provides insights into what food resources the larvae may have access to during a long-distance vertical migration, by allowing us to know how temperature-influenced larval physiology impacts their expended energy and if they need to feed during a migration through the dynamic food environments of a water column (*e.g.*, food-poor in the deep and food-rich at the surface).

Methods

Migration model

The energetic migration model (equation 1) developed by Young et al. (1996) calculates the cumulative expended energy of a vertically swimming larva.

$$E_t = \int_{t_0}^{t} KQ_0 e^{-rmvt}\, dt \tag{1}$$

Integrating the migration model with respect to time yields:

$$E_t = \left(\frac{-KQ_0}{rmv}\right) e^{-rmvt} - \left(\frac{-KQ_0}{rmv}\right) e^{-rmvt_0} \tag{2}$$

where E_t is the cumulative expended energy in units of Joules and K is a conversion factor for energy units. I used the average of the oxyenthalpic equivalent for proteins, lipids, and carbohydrates (0.00048 mJ pmol O_2^{-1}, Gnaiger, 1983) for K because the exact metabolic substrate is unknown. Several input variables for the model, including the rate of change of the temperature of the water column as a function of depth (m) in °C meter^{-1}, the vertical swimming velocity of the larvae (v) in meters hour^{-1}, and the initial rate of metabolism (Q_0) in pmol O_2^{-1} hour^{-1} larva^{-1}, and the rate of change of metabolism as a function of water temperature (r) in pmol O_2^{-1} hour^{-1} larva^{-1} °C^{-1} were determined experimentally. Finally, (t) is time in hours, and (t_0) is the starting time of migration corresponding to a water depth and temperature.

Sample collection and animal husbandry

During a June 2021 expedition of the R/V *Thomas G. Thompson*, *T. naticoidea* egg capsules on mussel shells were collected with the ROV Jason at approximately 650 meters depth

from the Brine Pool NR1 cold-seep (27.7236771 N, -91.2793722 W, Figure 1) off the coast of Louisiana in the Gulf of Mexico. A water temperature profile was obtained using a Conductivity, Temperature, and Depth (CTD) device on the same day the egg capsules were collected. When returned to the ship, the egg capsules were held in filtered seawater in a cold room at 6°C.

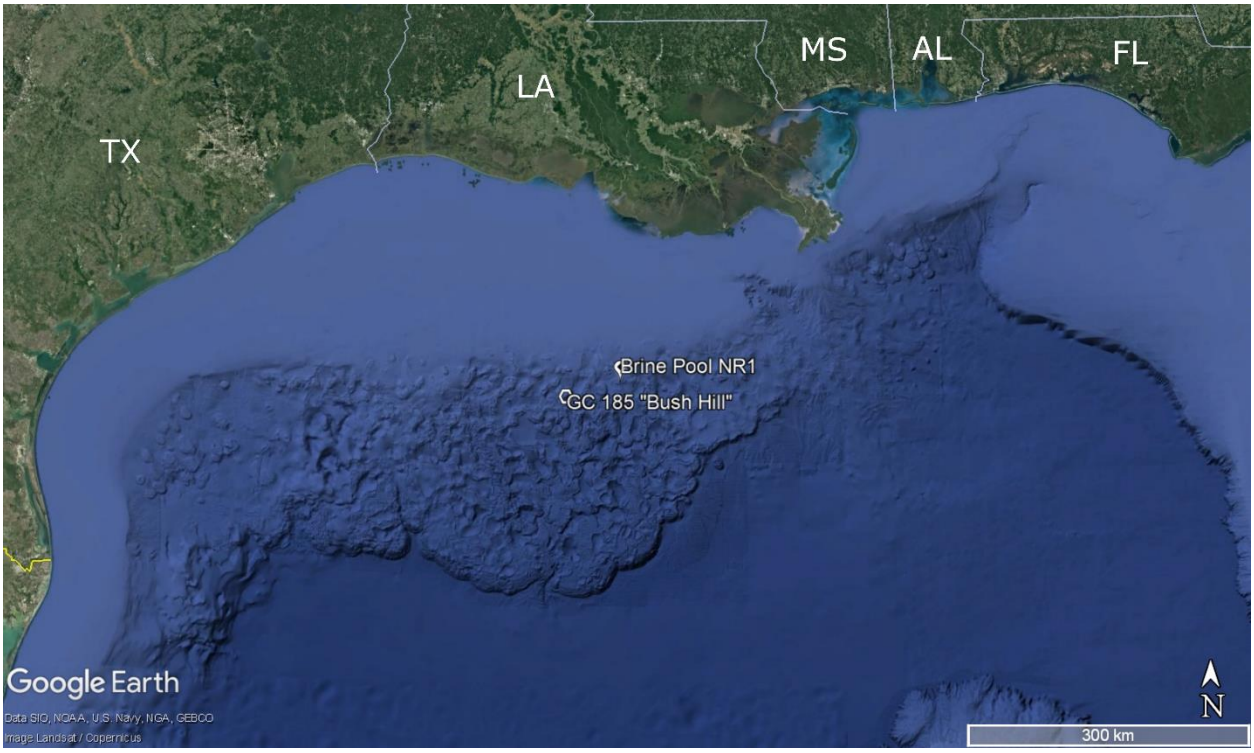

Figure 1 – Location of the Brine Pool NR1 study site off the coast of Louisiana in the Gulf of Mexico. GC 185, a.k.a. Bush Hill, is also provided for reference. The scale bar in the bottom right corner of the image is 300 km. Image taken from Google Earth Pro version 7.3.6.9345.

The egg capsule samples were collected on June 13, 2021. Seven days later at the end of the research cruise, the egg capsules were shipped overnight to Shannon Point Marine Center in Anacortes, WA where they were partitioned into well plates filled with chloramphenicol-treated filtered seawater. Chloramphenicol is an antibiotic, and when used at concentrations of 0.5 to 25 $\mu g\ mL^{-1}$, is suitable for use with gastropod larvae (Strathmann, 1987) and has been shown to increase survival and development of encapsulated *T. naticoidea* larvae in culture (Van Gaest, 2006). The water in the well plates was changed three times per week. The well plates of egg capsules were stored in a 6°C incubator.

The egg capsules were examined daily for hatching larvae. A total of 172 egg capsules were first placed into the incubator on June 21, 2021, and two days later larvae began to hatch. When the larvae hatched, they were carefully collected with a Pasteur pipette and stored in a separate well plate with the same chloramphenicol-treated filtered seawater. The water for the larval cultures was changed daily. The larvae were then allocated for one of the three aspects of this project: the swimming experiment, the respiration experiment, or calorimetry measurements.

Swimming experiment

For the swimming and respiration experiments, a range of temperatures was chosen to represent the water column temperatures that the larvae might experience during a vertical migration in the Gulf of Mexico in the month of June. The lowest temperature of 6°C is the temperature of the water at the Brine Pool where the samples were collected. The highest temperature of 31°C was chosen because this is near the upper bounds of the thermal tolerance of the larvae (Van Gaest, 2006), and surface temperatures in the Gulf of Mexico can reach this value in the summer months (Arellano & Young, 2011; Flögel & Dullo, 2011). The middle

temperatures of 12, 17, and 24°C were chosen with a random number generator (*random.org - True Random Number Service*, 1998).

The walk-in incubator at SPMC was used for the swimming experiment. To ensure that the temperature of the room was in line with the treatment levels, 2 liters of aerated filtered sea water were placed inside the room and monitored with an analog alcohol thermometer (Table 1). Experiments were conducted in the dark to avoid any phototaxis response from the larvae.

Table 1 – Temperature measurements, external digital temperature display and internal analog alcohol thermometer, for the SPMC walk-in incubator during the June 30, 2021, larval swimming experiment. The internal thermometer was placed inside a 2-liter container of water. The temperature treatments for the swimming experiment were planned to be 6, 12, 17, 24, and 31°C.

External, digital displayed temperature (°C)	Internal, analog thermometer temperature (°C)
5.8	5.5
12.0	11.9
17.0	16.8
24.0	23.6
31.3	30.5

The larvae for the swimming experiment hatched from egg capsules on June 25, 2021, and five days later they were placed into rectangular 4.5-mL polystyrene cuvettes for filming (1.2 cm x 1.2 cm x 4.5 cm height). A total of 300 larvae were used for the swimming experiment. The larvae were first pooled into a small beaker filled with air-saturated, filtered sea water. The larvae were then selected from this pool and placed into cuvettes filled with the same air-saturated filtered sea water. Fifteen replicate cuvettes in total were each filled with twenty larvae.

It is important to note that the cuvettes of larvae were not filmed in a random order nor were they randomly assigned to a temperature treatment. Every cuvette of larvae was sequentially exposed to all five temperature treatments: 6, 12, 17, 24, and 31°C. The cuvettes were all filmed consistently and sequentially from cuvette number one to cuvette number fifteen across each temperature treatment. The larvae were initially placed into the dark room at a treatment temperature for an hour prior to their filming. After filming, the temperature of the room was raised to the subsequent higher temperature. It took about an hour for the room and the 2 liters of water within the room to come up to the next temperature, and during this time the larvae are adjusting in the cuvettes inside the room. The 2 liter container of water was used as a thermal mass to approximate the temperature within the cuvettes. This cycle of filming and larval adjusting, while the temperature of the room increased for the next treatment, was repeated for the five temperatures, and took a little over eight hours to complete. The water within the cuvettes was not replenished or changed during the approximately eight-hour filming session, and oxygen concentration in the cuvettes was not measured. The larvae in the cuvettes were not exposed to limited oxygen concentrations during filming due to the respiration rates determined later in this study.

The cuvettes were backlit with an infrared light and filmed in the dark with an infrared sensitive camera (Imaging Development Systems, uEye model UI-5240CP-NIR-GL) using a small depth-of-field zoom lens (Edmund Optics, 10x CFZoom, 8.5-90mm, f -2.5, model R5000266480-16029) inside the walk-in incubator. The distance between the center of the cuvettes and the camera lens was kept constant at 25 cm. This provided a large enough field of view for the camera to simultaneously record three cuvettes: two cuvettes with larvae and an empty, scale cuvette. The scale cuvette was used in the video analysis and had vertical measurements in 5 mm increments to calibrate the subsequent video analysis.

After all filming had been completed, the videos were analyzed following a three-step protocol. First, the videos were calibrated, and the contrast was adjusted using Lab View Software (National Instruments 2014, Service Pack 1, version 14.0.1). The software processed the frames of the videos, tracking the larvae, and creating track files containing coordinate data. Second, the coordinate track data were analyzed with MatLab (MathWorks, R2014a version 8.3.0.532) using a script written by Staats et al. (2009). The script used a nearest-neighbor algorithm that paired particles of similar locations in space and time to generate a swimming path for the larvae. The method of using Lab View and MatLab to analyze larval swimming behavior is similar to that in Wheeler et al. (2013). However, I did not account for any three-dimensional aspects of the swimming path (*e.g.*, larvae swimming front to back relative to the camera within the cuvette) because I only had one camera with a fixed field of view and did not use a laser sheet.

Finally, the swimming tracks of larvae were manually reviewed and proofed using a separate Lab View program. To avoid edge effects of the cuvette, only vertically swimming larvae tracks in the middle of the cuvette were selected for analysis. To be used, a track needed

to be greater than five millimeters from the bottom or top meniscus of the cuvette, and greater than two millimeters (about 3 to 4 body lengths, assuming a larval body length range of 0.585 to 0.726 mm, Van Gaest, 2006) from the lateral sides of the cuvette. While the goal was to collect five swimming tracks of larvae per cuvette, some cuvettes did not have five swimming tracks that fit the above selection criteria and fewer tracks were used in those instances. The vertical swimming velocities of the larvae were analyzed as a function of the water temperature.

Respiration experiment

Respiration of the larvae was measured by placing the larvae into autoclaved filtered seawater in 1.75 mL vials with PreSens oxygen sensing spots (PreSens GmbH, batch number 191217-101_PSt3-111-02). A PreSens Fibox 4 oxygen meter was calibrated for each of the five temperature treatments of the experiment: 6, 12, 17, 24, and 31°C. The salinity of the autoclaved filtered sea water, measured with a refractometer, was 31 ppt. The atmospheric pressure in Anacortes, WA, on the day of the experiment was 1022 mbar.

The larvae for the respiration experiment hatched on September 21, 2021, and nine days later they were used in the experiment. The age of the larvae post-hatching was similar to the age of larvae I used for the swimming experiment. The larvae were pooled in a beaker with fully aerated, autoclaved filtered sea water. Six larvae were then placed into each of the 25 individual vials used for the five temperature treatments for a total of 150 larvae. The oxygen sensing spot vials, both the larvae- and blank-vials, were filled with the same autoclaved filtered sea water from the beaker pool.

Thirty-five vials with oxygen sensing spots were used for the experiment. There were seven vials used for each temperature treatment: five vials contained larvae and two vials were blanks with no larvae. The vials were gently rotated prior to measuring the oxygen concentration

within to help avoid oxygen stratification during the experiment, and a two-millimeter glass bead was placed into the blank vials to help agitate the water in lieu of larvae. The seven vials per temperature treatment were placed into independent water baths for the five temperature treatments. The five water baths were in a dimly lit room and had lids for their water bath chambers to reduce light exposure. The seven vials in each temperature treatment were adjusted to the water baths for thirty minutes before the first measurement of oxygen concentration.

Oxygen concentration was measured in two-hour intervals in units of percent air saturation until the vials decreased by 20% air saturation. The 6 and 12°C vials were measured over a 28-hour period. The 17°C vials were measured over a 26-hour period. The 24 and 31°C vials were measured over a 24-hour period.

The respiration data for the five temperature treatments were compiled and the respiration rates were calculated. Any values below the relative 80% air saturation were disregarded. This is a general rule but depends on the species, because below this value the larvae are stressed and are not respiring normally in their environment (Ikeda et al., 2000). Except in the 6°C treatment, the respiration rate in the blank vials was always less than the respiration rate within the vials with larvae (see Appendix Figures A and B).

The total oxygen concentration in the sea water was calculated in units of picomoles per liter accounting for the daily atmospheric pressure, the vapor pressure of the water corresponding to the temperature treatment, and the temperature dependent oxygen capacity of the water. Finally, combining these data with the size of the vial that the larvae were respiring in, and the total number of larvae per vial, the average individual respiration rate of the larvae in the vial was calculated.

Data from a previous experiment conducted by S.M. Arellano in 2014 following similar methods of measuring the respiration rate of *T. naticoidea* larvae in 1.75 mL vials with PreSens oxygen sensing spots and a PreSens Fibox 3 oxygen meter was used to augment the data collected in this study. The temperature treatments from the 2014 experiment were 4, 8, and 21°C. Five vials were used for each of the three temperature treatments; four vials had five larvae each and one vial was a control blank with no larvae. The 2014 data provided information to determine the rate of respiration of the larvae at a broader range of water temperatures. The respiration rates for these data are shown in Appendix Figure C.

Analysis and model fitting

A visual inspection of the CTD data with R (RStudio version 2022.07.0+548, utilizing R version 4.2.1) revealed that water temperature as a function of water depth had a distinct non-linear pattern. Thus, an exponential regression was applied to the data to determine the rate of change of the water temperature for inclusion in the migration model. The exponential regression model was fit to the CTD data, and the model was cross-validated 10 times with the caret package (version 6.0-92) to ensure an appropriate fit.

A linear mixed model was used to analyze the swimming experiment with R using the nlme package (version 3.1-157). I chose this approach because I filmed the cuvettes of larvae consistently and sequentially across all temperature treatments. To account for any variation between individual cuvettes and to make inferences about *T. naticoidea* larval swimming velocities, I designated the cuvettes as a random predictor. First, a generalized least squares model of vertical swimming velocity as a function of the fixed predictor of water temperature was compared to two linear mixed models: including fixed factor of temperature, and 1) random intercepts for the replicate cuvettes nested within temperature, and 2) random intercepts and

slopes for the cuvettes across temperatures. The three models were compared with the Akaike Information Criteria, and the most parsimonious model was chosen. The model fit was verified by visually inspecting the residuals and quantile-quantile plot (see Appendix Figures D and E) and cross-validated 10 times with a custom-built loop function. While there was a possibility of repeated sampling of individual larvae between temperatures, there was no way to track individual larvae or account for them in the model, so no adjustment was made for that potential lack of independence.

The 6°C temperature treatment did not yield detectable changes in respiration, and the blank vials had a higher rate of respiration than the larvae vials (Appendix Figure B), thus the 6°C treatment was removed from the analysis. The respiration rates collected in this study in 2021 (Appendix Figure A) were similar to the respiration rates collected by Arellano in 2014 (Appendix Figure C). The combined respiration rate data were initially visually inspected with R, and Loess smoothing was applied to assess any trends in the data. The Loess smoothing showed a non-linear trend reaching a maximum point at 21°C before decreasing and plateauing at 24 and 31°C. This turning point in the respiration rate can indicate stress after an optimal temperature (Miller & Stillman, 2012). Thus, I chose to focus on the data up to the maximum point in the respiration rate data. Because the migration model assumes an Arrhenius-style relationship between larval respiration rate and temperature (Young et al., 1996), I fit an exponential model to the data and cross-validated the final model 10 times with the caret package (version 6.0-92).

Migration model: putting the pieces together

The cumulative energy expended by a vertically swimming larva was calculated using the migration model from Young et al. (1996) with the rate of temperature change with water depth,

the experimentally measured mean vertical swimming velocity, and the temperature-dependent respiration rate. The vertical migration model was evaluated at discrete time intervals corresponding to vertical distance bins that represented the distance larvae could travel in a day of swimming. As larvae travel through the water column the water temperature changes, thus changing the base respiration rate, and this change is accounted for with the starting water depth and temperature of the vertical distance bins. Furthermore, the migration model was evaluated at three different vertical swimming velocities and three different distance bins corresponding to the different velocities (*i.e.*, the vertical velocity would change the distance the larvae travel in a day of swimming). The three velocities were: 1) the mean minimum velocity based on the ten lowest measured velocities, 2) the grand mean across all swimming velocities, and 3) the mean maximum velocity based on the ten highest measured velocities. Finally, the migration model was evaluated with a Shiny app that was created to compute the definite integral. The app is available for public use online at https://mitchell-hebner.shinyapps.io/LarvalEnergyIntegralApp/.

Calorimetry

Calorimetry was performed on newly hatched *T. naticoidea* larvae to compare the energy content of larvae to the model results for the cumulative energy expended by swimming larvae. Comparing the initial energy reserves of the larvae after they hatch with the model prediction could elucidate whether the larvae have the energy reserves to complete a long-distance vertical migration, or if they need to feed during their journey to the surface waters of the Gulf of Mexico.

*T. naticoidea l*arvae from two cruises to the Gulf of Mexico were used for calorimetry. The larvae were collected from two sites in the Gulf during March 2020 and from one site during June 2021. The number of larvae and the site locations are in Table 2. The collection and animal

husbandry protocol were identical for snails and egg capsules from both cruises, as previously described. Larvae were collected for calorimetry and prepared for cold storage within 2 days of hatching. Larvae were removed from the well plates with pipettes, counted, and placed into cryovials to be rinsed with a filtered 3% ammonium formate solution (Jaeckle & Manahan, 1989). Samples from cruise TN391 (June 2021) hatched approximately three months later and were immediately frozen and stored at -80°C. Samples from cruise AT42-24 (March 2020) hatched approximately seven to eight months later and were frozen and stored at -20°C (Table 2).

Table 2 – Number of larvae collected from sample sites during two cruises. Brine Pool and Bush Hill locations are shown in Figure 1. Storage date is the day that the larvae were collected and placed into a cryovial for cold storage. The storage date is no more than 48 hours after a hatching event.

Collection Site	Storage Date	Number of Larvae
R/V Atlantis AT42-24		
Brine Pool	26 Oct. 2020	100
	26 Oct. 2020	180
	29 Oct. 2020	127
	No date label	500
Bush Hill	30 Oct. 2020	59
	1 Nov. 2020	133
	9 Nov. 2020	
	11 Nov. 2020	218
	16 Nov. 2020	36
Brine Pool plus Bush Hill	15 Nov. 2020	89
No site label	No date label	70
R/V Thomas G. Thompson TN391		
Brine Pool	21 Sep. 2021	205
	Total Larvae	1,793

Prior to combustion in a Parr semi-micro bomb calorimeter (Parr Instrument Company, Precision thermometer model 6772, Semi-micro calorimeter model 6725, Semi-micro Oxygen bomb model 1109A), the larvae samples were lyophilized under a vacuum at -60°C for 48 hours using a FreeZone-1 lyophilizer (Labconoco, benchtop freeze dry system number 7740020). This process removed any excess water that could impact the gross heat calculation performed by the Parr calorimeter. During the 48 hours of lyophilization, the calorimeter was calibrated with a benzoic acid standard and met the threshold for acceptable calibration. The calibration combustion runs are shown in Appendix Table A.

The calorimeter required a mass of sample in the range of 0.02 – 0.2 grams for accurate measurement. The individual vials of larvae did not contain enough mass to meet the requirement of the calorimeter. To address the low sample mass, all 1,793 larvae (Table 2) were combined into one sample, and their total mass of 0.0013 grams was used for calorimetry. The larvae were pressed into a pellet with 0.0937 grams of benzoic acid to achieve sufficient mass for combustion. The mass of the benzoic acid was not predetermined, rather a result of the pellet pressing process. The pellet press was 5 mm in diameter. A small amount of benzoic acid was added to the press and tamped down. Then the larvae were added to the press and more benzoic acid was placed atop the larvae, sandwiching the larvae between layers of benzoic acid. The pellet was tamped down and weighed. The mass of the larvae was subtracted from the final mass of the pellet to yield the mass of the benzoic acid. The pellet with combined larvae and benzoic acid was combusted following standard procedure for the Parr semi-microbomb calorimeter. Only one pellet of larvae was combusted, and because of this, the data were not analyzed statistically.

Results

CTD results

The CTD data collected above the Brine Pool in June 2021 showed water temperature as a function of water depth had a strong fit to an exponential regression model ($R^2 = 0.98$, Figure 2). A weak thermocline for this depth profile extended from the surface to approximately 50 meters (Figure 2).

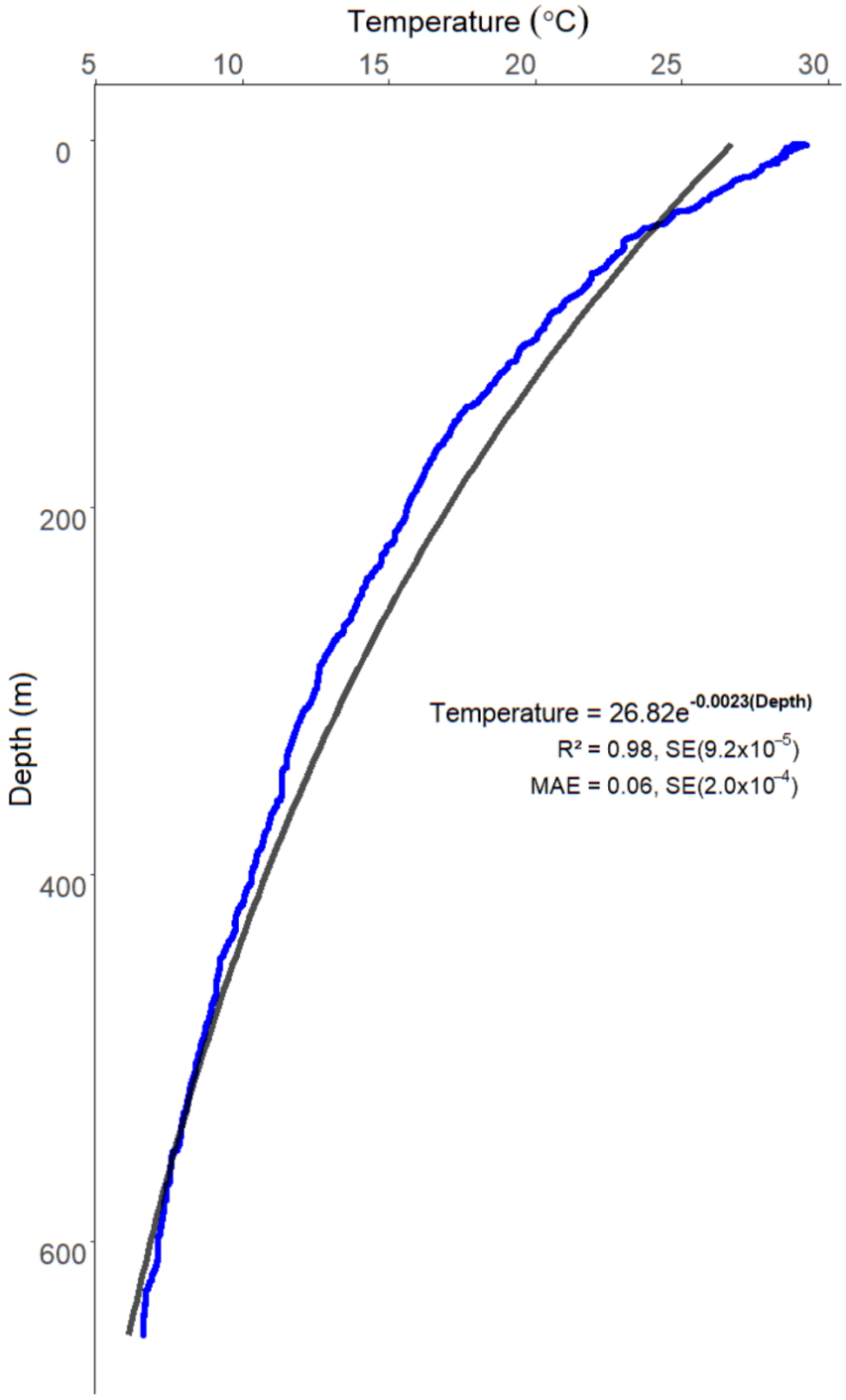

Figure 2 – Vertical profile of temperature (°C) above the Brine Pool location in June 2021 (blue line). The final model (black line), water temperature as a function of depth, was cross-validated 10 times. MAE is the mean absolute error in °C. SE is the standard error of the cross-validated model parameters.

Swimming experiment results

The mean vertical swimming velocities for 6, 12, 17, 24, and 31°C were ($\bar{x}$ ± 1 Standard Error) 0.42 $\pm$ 0.03 mm s^{-1}, 0.41 $\pm$ 0.03 mm s^{-1}, 0.36 $\pm$ 0.04 mm s^{-1}, 0.32 $\pm$ 0.05 mm s^{-1}, and 0.42 $\pm$ 0.04 mm s^{-1}, respectively (Figure 3). A linear mixed model with random intercepts for each replicate cuvette nested within temperature was the most parsimonious model fit to the swimming velocity data. However, water temperature did not appear to affect the vertical swimming velocities of the *T. naticoidea* larvae ($p = 0.59$, Mean conditional $R^2 = 0.088$, Table 3). A comparison of this parsimonious model to other models attempted to fit to these data are shown in Appendix Table B. The vertical migration model was evaluated using an overall mean of all vertical swimming velocities of 1.43 ± 0.06 m $hour^{-1}$, a mean of the ten lowest minimum vertical velocities of 0.66 ± 0.04 m h^{-1}, and a mean of the ten highest maximum vertical velocities of 2.22 ± 0.09 m h^{-1}.

Table 3 – Structure of the most parsimonious linear mixed model for the vertical swimming velocity data.

Fixed effects					
Parameter	Estimate	SE	DF	t	p
Intercept	0.42	0.04	143	11.12	< 0.001
Temperature	-0.001	0.001	143	-0.54	0.59
Random effects					
Random intercepts for each replicate cuvette nested within temperature					
k-fold cross-validation results (k = 10)					
Mean conditional R^2 = 0.088 ± 0.034			Mean Absolute Error = 0.16 ± 0.01 mm s^{-1}		

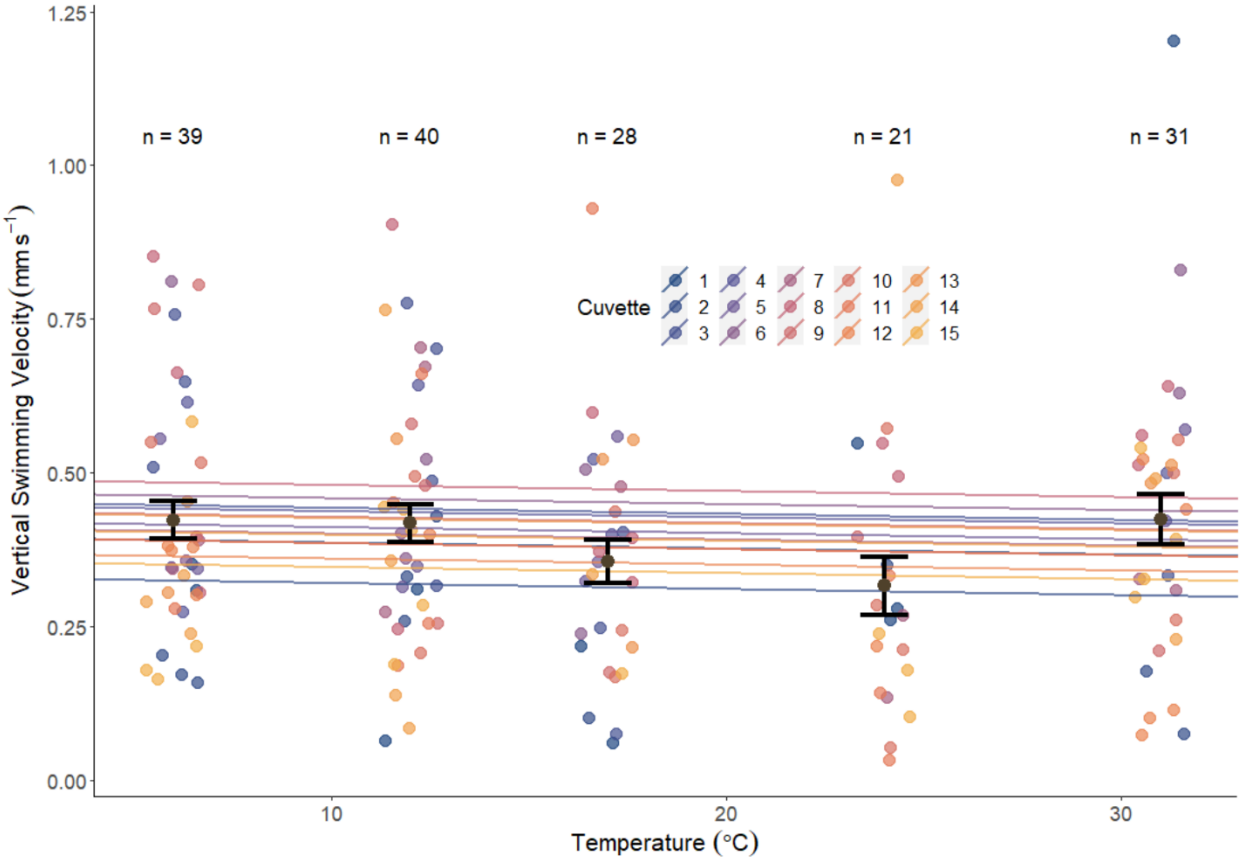

Figure 3 – Plot of individual vertical swimming larval tracks for each temperature treatment: 6, 12, 17, 24, and 31°C. Data points are horizontally jittered for increased visibility. The color represents the replicate cuvettes, and lines from the random intercepts for each cuvette across temperature. Mean values are shown for the temperature treatments with error bars representing the standard error. The number of individual swimming tracks is represented by the sample size above each temperature treatment. Colors are from PNWColors R-package (Lawlor, 2020).

Respiration experiment results

The 6°C treatment data were removed because the rate of respiration in the blank vials were higher than the rate of respiration for the larvae vials (Appendix Figure B), and data from 2014 measurements by Arellano were combined with my measurements. Loess smoothing to the data indicated that the maximum, or the turning point of the respiration rate data, occurs at a temperature of 21°C (Figure 4). This may be the *pejus* temperature, which is defined as the maximum temperature within the thermal optimum window (Miller & Stillman, 2012). Beyond the *pejus* temperature the larvae are believed to be experiencing metabolic stress, indicated by the decline in the respiration rate and the plateau at 24 and 31°C (Figure 4). The mean respiration rates found in this study are ($\bar{x}$ ± 1 Standard Error) 86.2 ± 8.8 pmol O_2 $hour^{-1}$ $larva^{-1}$, 142 ± 44.1 pmol O_2 $hour^{-1}$ $larva^{-1}$, 470 ± 32.8 pmol O_2 $hour^{-1}$ $larva^{-1}$, 765 ± 52.9 pmol O_2 $hour^{-1}$ $larva^{-1}$, 1680 ± 262 pmol O_2 $hour^{-1}$ $larva^{-1}$, 857 ± 76.8 pmol O_2 $hour^{-1}$ $larva^{-1}$, and 1201 ± 46.9 pmol O_2 $hour^{-1}$ $larva^{-1}$ at 4, 8, 12, 17, 21, 24, and 31°C, respectively (Figure 4). The non-linear pattern up to the *pejus* temperature was confirmed by comparing models evaluated by Akaike Information Criterion (Table 4). Respiration and energy consumption up to the *pejus* temperature of 21°C are exponentially related and temperature is a significant predictor of respiration rates and energy consumption ($p < 0.001$, $F_{1,20} = 159$, $R^2 = 0.97$, Figure 5).

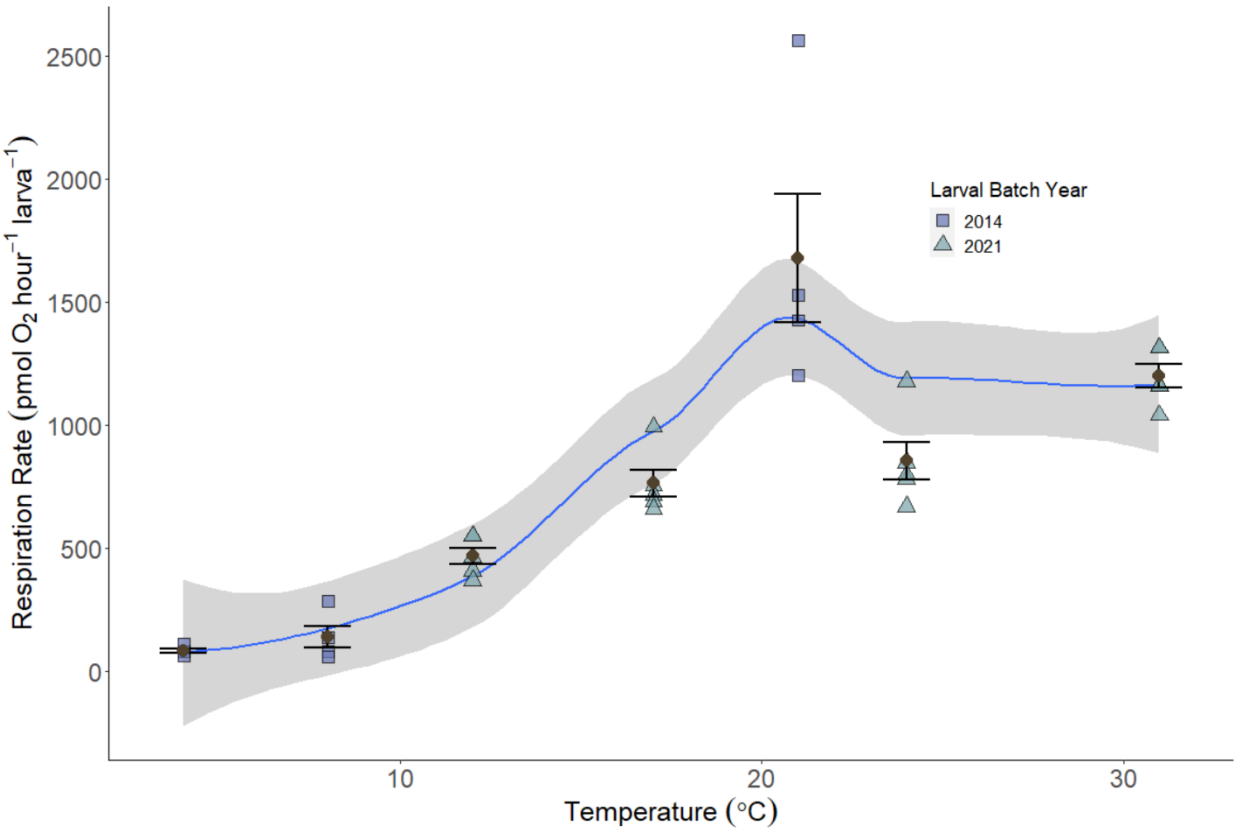

Figure 4 – Initial visual inspection of the combined respiration rate data from 2014 and 2021. Data points are the average respiration within the replicate vials of larvae. Loess smoothing is applied to the data to determine a trend. The shaded region around the blue line is the 95% confidence interval for the data smoothing. The temperature treatments are 4, 8, 12, 17, 21, 24, and 31°C. Brown dots represent the mean respiration rate of the vials of larvae for different temperatures. Error bars represent the standard error of the mean. Colors of the data points are from the PNWColors package (Lawlor, 2020).

Table 4 – Linear and non-linear model comparison with Akaike Information Criteria for the respiration rate as a function of temperature.

Model	AIC
Respiration rate ~ Temperature	474.3
Respiration rate ~ $e^{Temperature}$	59.7

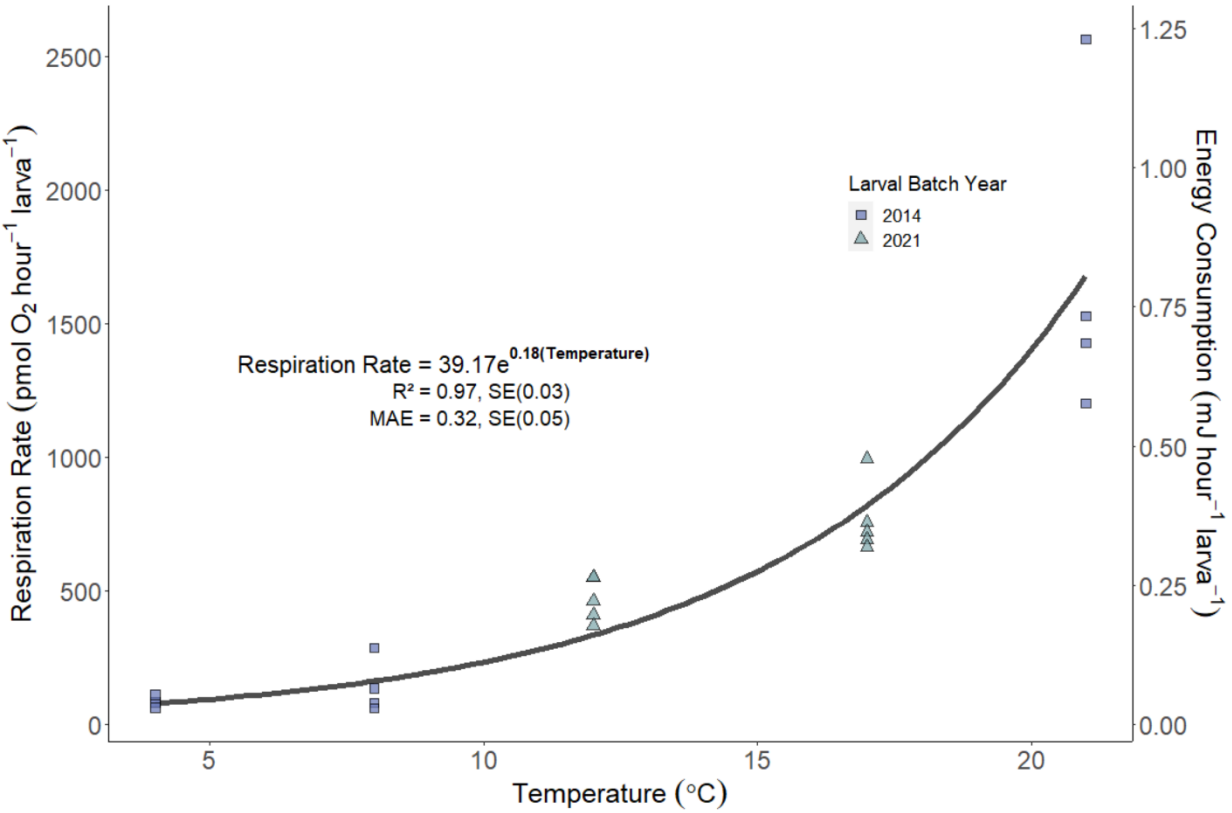

Figure 5 – Respiration rate of the larvae in pmol O_2 $hour^{-1}$ $larva^{-1}$ up to the *pejus* temperature of 21°C. Each data point represents the average respiration rate within a vial of larvae. Energy consumption rates of the larvae are converted from the respiration rate knowing 0.00048 mJ pmol O_2^{-1}. The final exponential model was cross-validated 10 times. MAE is the mean absolute error in units of pmol O_2 $hour^{-1}$ $larva^{-1}$. Colors of the data points are from the PNWColors package (Lawlor, 2020).

Migration model output

Integrating the Young et al. (1996) vertical migration model with respect to time yields:

$$E_t = \left(\frac{-KQ_0}{rmv}\right)e^{-rmvt} - \left(\frac{-KQ_0}{rmv}\right)e^{-rmvt_0} \quad (2)$$

where E_t is the cumulative expended energy in units of Joules, K is the average of the oxyenthalpic equivalent for proteins, lipids, and carbohydrates (0.00048 mJ pmol O_2^{-1}, Gnaiger, 1983), (m) is the rate of change of the temperature of the water column as a function of depth in °C meter^{-1}, (v) is the vertical swimming velocity of the larvae in meters hour^{-1}, (Q_0) is the initial rate of metabolism in pmol O_2^{-1} hour^{-1} larva^{-1}, and (r) is the rate of change of metabolism as a function of water temperature in pmol O_2^{-1} hour^{-1} larva^{-1} °C^{-1}. Finally, (t) is time in hours, and (t_0) is the starting time of migration corresponding to a water depth and temperature.

The equation from the exponential regression of the CTD:

$$Temperature(°C) = 26.82e^{-0.0023(Depth\ (meters))} \quad (3)$$

gives m, the rate of change of the water temperature as a function of depth (-0.0023 °C m^{-1}).

The vertical swimming velocity (v) was assumed to be constant, and the model was evaluated at the mean minimum velocity for the ten lowest values of 0.66 m h^{-1}, the mean velocity for all values of 1.43 m h^{-1}, and the mean maximum velocity for the ten highest values of 2.22 m h^{-1}. The vertical migration model was evaluated at discrete depth bins which corresponds to the distance the larvae can swim in one day at each of the three swimming velocities.

The equation from the exponential regression of the respiration rate:

$$Respiration\ rate\ (pmol\ O_2\ hour^{-1}\ larva^{-1}) = 39.17e^{0.18(Temperature\ (°C))} \quad (4)$$

gives Q_0 (39.17 pmol O_2 hour^{-1} larva^{-1} at 0°C) as the base respiration rate of the larvae at t_0, but t_0 is the starting time of migration corresponding to a depth and temperature, which may not be 0°C, and r is the rate of change of the respiration rate as a function of temperature (0.18 pmol O_2 hour^{-1} larva^{-1} °C^{-1}). The migration model was evaluated from the starting depth of 650.8 meters up to the *pejus* temperature depth of 87.7 meters because of the rate of change of larval respiration as a function of water depth was only evaluated up to 21°C (Figure 5), and more complex models like a quadratic or cubic regression are needed to capture the trend in the data above the *pejus* temperature (Figure 4).

The model predicted that an average larva swimming vertically from a depth of 650.8 meters to the photic zone (200 meters) at a constant mean minimum velocity of 0.66 ± 0.04 m h^{-1} would expend 111.7 mJ in 28.6 days (Figure 6a). A larva swimming vertically through the same depth range at a constant mean velocity of 1.43 ± 0.06 m h^{-1} would expend 52.7 mJ in 13.5 days to reach the photic zone (Figure 6b). Finally, a larva swimming vertically at a constant mean maximum velocity of 2.22 ± 0.09 m h^{-1} would expend 31.6 mJ in 7.7 days to reach the photic zone (Figure 6c).

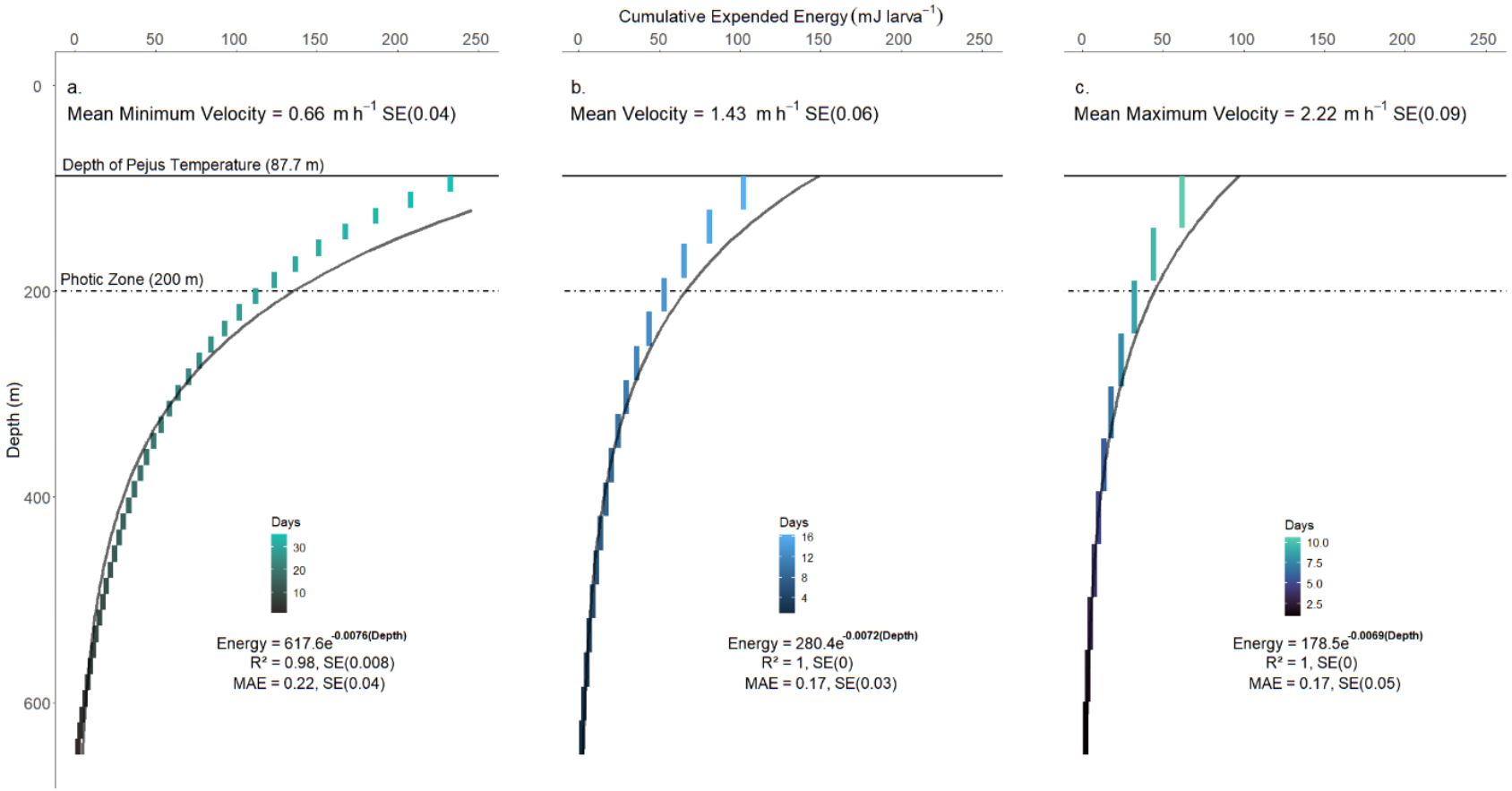
Cumulative Expended Energy (mJ larva^{-1})
0
50
100
150
200
250
Depth (m)
0
200
400
600
a.
Mean Minimum Velocity = 0.66 m h^{-1} SE(0.04)
Depth of Pejus Temperature (87.7 m)
Photic Zone (200 m)
Days
30
20
10
Energy = 617.6e$^{-0.0076(Depth)}$
R² = 0.98, SE(0.008)
MAE = 0.22, SE(0.04)
b.
Mean Velocity = 1.43 m h^{-1} SE(0.06)
Days
16
12
8
4
Energy = 280.4e$^{-0.0072(Depth)}$
R² = 1, SE(0)
MAE = 0.17, SE(0.03)
c.
Mean Maximum Velocity = 2.22 m h^{-1} SE(0.09)
Days
10.0
7.5
5.0
2.5
Energy = 178.5e$^{-0.0069(Depth)}$
R² = 1, SE(0)
MAE = 0.17, SE(0.05)

Figure 6 – Migration model output evaluated at three different swimming velocities: minimum of 0.66 m h^{-1}, mean of 1.43 m h^{-1}, and a maximum of 2.22 m h^{-1}. Each data point represents the vertical distance bin that a vertically swimming larva would travel in approximately one day of constant swimming: minimum of 15.6 m, mean of 33.1 m, and a maximum of 51.2 m. The solid black line representing the *pejus* temperature of 21°C corresponds with 87.7 meters depth, based on CTD data collected in this study, and the respiration data was evaluated up to the *pejus* temperature. The dashed line represents the photic zone depth at 200 meters. The final model for each swimming velocity, cumulative expended energy in mJ as a function of water depth in meters, was cross-validated 10 times. MAE is the mean absolute error in mJ $larva^{-1}$. Colors for panel a are from PNW Colors (Lawlor, 2020). Colors for panel b are from base R. Colors from panel c are from viridis package (version 0.6.2).

Calorimetry results

The combustion of the single pellet with 0.0013 grams of larval sample plus the 0.0937 grams of benzoic acid yielded a gross heat of combustion of -1,491.3 calories $gram^{-1}$ (Table 5). Since the gross heat of combustion is a negative value, something clearly went wrong in the processing of the sample, so the caloric content of an individual larva was not considered.

Table 5 – Calorimeter combustion of the larval sample. The heat of combustion of the benzoic acid standard used was 6318 cal g^{-1}. The fuse value is the number of calories that are consumed by the combusted wire. The acid value is the number of calories extracted from the bomb system due to formation of nitric acid via combustion. The Energy Equivalent (EE) value is calculated by the Parr thermometer.

Sample ID	Initial Temp (°C)	Jacket Temp (°C)	Temp rise (°C)	Sample mass (g)	Fuse (cal)	Acid (cal)	EE value (cal $°C^{-1}$)	Gross Heat (cal g^{-1})
40	20.0178	21.8250	1.2742	0.0013	15.0000	10.0000	482.745	-1491.3

Discussion

The goal of my study was to evaluate how the swimming and metabolic rates of *T. naticoidea* larvae are influenced by water temperature and use these rates as empirically derived parameters to evaluate the migration model from Young et al. (1996) to determine how much energy the larvae would expend while vertically swimming toward the photic zone. Larval respiration rate was influenced by the water temperature with a possible *pejus* temperature at 21°C, corresponding to 87.7 m depth above the Brine Pool cold-seep in June 2021. The *pejus* water temperature and depth will vary across seasons in the Gulf of Mexico. I found that the larvae exhibit a mean vertical swimming velocity of 1.43 ± 0.06 m h^{-1} and could swim to the photic zone (200 m depth) within 13.5 days from the start of their migration, expending 52.7 mJ of energy along their way. The 13.5 days to reach the photic zone is within the range of 16 days that the larvae can swim without eating (Van Gaest, 2006). However, without a measurement of the initial energy reserves that the larvae have after they hatch, I am unable to confirm if the larvae could reach the photic zone without feeding during their vertical migration.

Implications of a vertical migration for feeding T. naticoidea

The surface waters are food-rich while the deep-sea is food-poor, and a larva undergoing a vertical migration to food-rich waters would need sufficient energy reserves to reach the photic zone or would need to feed during the migration. However, there are limited studies that have collected the energy values of marine invertebrate larvae and eggs, thus making comparisons and inferences difficult between my work and others. My study found *T. naticoidea* larvae that swim vertically at a mean velocity would expend 52.7 mJ of energy to reach the photic zone (Figure 6b). Jaeckle and Manahan (1989) examined the energy content of the lecithotrophic larvae of *Haliotis rufescens* with proximate biochemical analysis and found that newly developed larvae

have an energy content of 42.35 mJ. This value is similar to the cumulative expended energy of *T. naticoidea* but is relatively higher than some bryozoan larvae (Table 6). The energy values collected in my study are comparable, but more data is needed on the energy content of a variety of marine invertebrates to enable more rigorous comparisons.

Table 6 – Comparison of energy values from eggs and larvae of three phyla and eleven species. *T. naticoidea* and *G. childressi* are the only deep-sea organisms. * is the cumulative expended energy while vertically swimming at a mean velocity, [1] is standard error, [2] is standard deviation.

Species	Phylum	Life-stage	Energy (mJ individual $^{-1}$)	Reference
Thalassonerita naticoidea	Mollusca	Larva	52.7*	My study
Haliotis rufescens		Larva	42.35	Jaeckle & Manahan (1989)
Bugula stolonifera	Bryozoa	Larva	5.0 ± 0.41^{1}	Wendt (2000)
Bugula simplex		Larva	10.7 ± 0.28^{1}	
Bugula neritina		Larva	33.7 ± 0.13^{1}	
Gigantidas childressi	Mollusca	Egg	2.95 ± 0.08^{2}	Arellano (2008)
Mytilus trossulus		Egg	1.85 ± 0.95^{2}	
Mytilus galloprovincialis		Egg	1.33 ± 0.05^{2}	
Clipeaster rosaceus	Echinodermata	Egg	76.0 ± 9.0^{2}	Zigler et al. (2008)
Clipeaster subdepressus		Egg	5.1 ± 0.5^{2}	
Brisaster latifrons		Egg	251.0 ± 48.0^{2}	

Moreover, deep-sea organisms are different from their shallow water relatives with regard to their respiration rates, and comparisons of *T. naticoidea* larval respiration rates to respiration rates of other molluscan larvae or different species are helpful to show that *T. naticoidea* larvae respire at greater rates (Table 7). My study found that *T. naticoidea* larvae have a large range of average respiration across temperatures (Figure 4). A study of gastropod veligers from Antarctica found that at -1°C *Marseniopsis mollis* and *Torellia mirabilis* respire at an average of 317 ± 14 pmol O_2 h^{-1} and 208 ± 11 pmol O_2 h^{-1}, respectively (Peck et al., 2006). The larvae of the Antarctic asteroid *Odontaster validus* at 2°C respires at a rate of 31.4 pmol O_2 h^{-1} $larva^{-1}$ (Peck & Prothero-Thomas, 2002). A study of 7-9 day old green abalone larvae, *Haliotis fulgens*, found respiration rates of 81.7 ± 5.9 pmol O_2 $hour^{-1}$ $larva^{-1}$ at 15°C (Moran & Manahan, 2003). The abalone larvae were of similar age to the *T. naticoidea* larvae in this study. The respiration values collected in my study are comparable to some respiration rates of other species, but as with the energy content of marine invertebrates, more data is needed regarding respiration rates to facilitate comparison.

Table 7 – Table of respiration rates of larvae from two phyla and five species from four studies, to compare to the range of respiration rates from my work. Errors are the standard error.

Organism	Phylum	Temperature (°C)	Mean respiration rate (pmol O_2 $hour^{-1}$ $larva^{-1}$)	Reference
Marseniopsis mollis	Mollusca	-1	317 ± 14	Peck et al. (2006)
Torellia mirabilis		-1	208 ± 11	
Haliotis fulgens		15	81.7 ± 5.9	Moran & Manahan (2003)
Odontaster validus	Echinodermata	2	31.4	Peck & Prothero-Thomas (2002)
Thalassonerita naticoidea	Mollusca	4	86.2 ± 8.8	My study
		8	142 ± 44.1	
		12	470 ± 32.8	
		17	765 ± 52.9	
		21	1680 ± 262	
		24	857 ± 76.8	
		31	1201 ± 46.9	

When the larvae swim to the photic zone, they could likely find suitable food to eat to support their development. In the Gulf of Mexico, phytoplankton concentrations change seasonally (Müller-Karger et al., 1991), and the community composition and biomass vary with water depth (Selph et al., 2021). During the summer months off the coast of Louisiana, the predominant phytoplankton assemblages may be *Prochlorococcus*, prymnesiophytes, prasinophytes, and other picophytoplankton (Selph et al., 2021). We know that *T. naticoidea* larvae are capable of eating phytoplankton because Van Gaest (2006) fed *T. naticoidea* larvae *Thalassiosira pseudonana* and *Isochrysis galbana* and imaged the algae in the larval gut. *I. galbana* is a haptophyte and a member of the clade that includes the prymnesiophytes. Moreover, Van Gaest (2006) found that the larvae continued swimming for 16 days after hatching. The migration model supported that the larvae can reach the photic zone (200 m depth) in 13.5 days of swimming (Figure 6b).

Based upon the model from Young et al. (1996), and assuming a mean vertical velocity of 1.43 m h^{-1}, *T. naticoidea* larvae are only exposed to phytoplankton after migrating vertically for 13.5 days (Figure 6b). From the start of their journey until approximately two weeks later, the larvae swim through water that has relatively low concentrations of food resources (Smith et al., 2008). Low food concentration can cause nutritional stress (Boidron-Métairon, 1995). Nutritional stress and starvation rates for larvae depend on many factors such as the individual species, the developmental stage, and water temperature (Anger & Dawirs, 1981). However, in food-poor environments, *T. naticoidea* might feed upon non-algal food sources. For example, Boidron-Métairon (1995) describes several sources of food that are not algae, such as bacteria and dissolved organic matter. While some bacteria can be hazardous at high concentrations, in low concentrations bacteria can improve growth of bivalve larvae (Boidron-Métairon, 1995).

Additionally, *Shinkailepas* sp., a deep-sea phenocopepalid slipper limpet and a neritoid relative of *T. naticoidea*, can feed on *Synechococcus* bacteria and retain large lipid deposits (Young et al. 2018). Finally, uptake of dissolved organic matter like amino acids and sugars can contribute a large fraction (30-50%) of the metabolic needs of larvae (Boidron-Métairon, 1995). Dissolved organic materials can be more than a supplementary avenue for food resources at many water depths because of the variety of dissolved organic materials present there (Boidron-Métairon, 1995). Future studies of these larvae, and other deep-sea species could benefit from understanding all avenues of food intake.

Seasonal environmental factors like currents and sea surface temperature can be influential for vertical migration potential of *T. naticoidea* larvae because the adults have a lengthy spawning season. Egg capsules are deposited in the greatest frequency from December to February and hatching has historically been reported to occur between March and July (Van Gaest, 2006). My study had late-season collection of egg capsules in June 2021 and hatching of larvae occurred through September 2021. *T. naticoidea* larvae are estimated to have a planktonic larval duration ranging from 8 to 12 months (Van Gaest, 2006). If any larvae were undergoing a late-season vertical migration *in situ* they would experience a different temperature profile and sea surface temperature in the photic zone of the water column because of the large seasonal variation of temperature within the Gulf (Arellano et al., 2014; Müller-Karger et al., 1991, 2015). Moreover, the chlorophyll concentrations observed by Müller-Karger et al. (2015) were near their lowest concentrations, approximately 0.14 mg m^{-3} in September within the region above the Brine Pool. Not only does the water temperature vary with seasons, but so does the phytoplankton concentration. This means that the *T. naticoidea* larvae that vertically migrate,

regardless of the season, will need to be adaptable to a range of water temperatures and must be able to assimilate food from a variety of sources.

The Gulf of Mexico is a unique oceanographic ecosystem because of ocean currents (e.g., the Loop Current and formation of eddies) and hurricanes that could create conditions that support the migration of *T. naticoidea* and other deep-sea larvae. The Loop Current has fragile boundaries and can shed anticyclonic eddies, and typically does so between June and September (this timeframe aligns with late-season hatching events). The interval for eddy shedding ranges from weeks to approximately 1.5 years, with an average shedding interval of eight to nine months (Hall & Leben, 2016). These eddies can cause an upwelling event to occur (Müller-Karger et al., 2015). Hurricanes during their travel across the Gulf can also cause upwelling events (Walker et al., 2005), and these typically appear between June and November (also, in alignment with late-season hatching). Upwelling events bring cold, nutrient-rich water closer to the surface leading to a decrease in sea surface temperatures and can create a phytoplankton bloom. If some lucky *T. naticoidea* larvae migrating vertically from the depths of the Gulf were caught in a Loop Current or hurricane-induced upwelling event, they could benefit in several ways. For example, the larvae could reduce their energy consumption by being carried to the surface via upwelling rather than by vertically swimming. Additionally, colder water temperatures would reduce their respiration and metabolism thereby allowing the larvae to swim closer to the surface and be exposed to dynamic surface currents. Finally, the larvae would have access to an increased phytoplankton supply due to a bloom driven by deep water nutrients.

Combining larval migration models with large-scale oceanographic models is imperative to elucidate locations where deep-sea benthic organisms may live so we can fully understand how the populations are related across space. Young et al. (2012) modeled the dispersal potential

of *T. naticoidea* larvae utilizing large-scale oceanographic models with the larvae beginning their dispersal near known habitat locations in the Gulf of Mexico, and from two different starting dispersal depths: 100 meters and 500 meters. The former depth of 100 meters is achievable by a vertically migrating larva as determined by my work and Arellano et al. (2014) collecting larvae at the surface. The latter depth of 500 meters is close to their natal depth of approximately 650 meters, but above the slow-moving deep-sea benthic boundary layer. The results of the modeling by Young et al. (2012) found that *T. naticoidea* larvae that begin their journey in the Gulf of Mexico at a starting depth of 500 meters will likely remain in the Gulf, and therefore have the potential for recruitment to local populations. The model also indicated that *T. naticoidea* larvae that reach 100 meters depth may also remain in the Gulf, but many larvae dispersing from this depth had a model trajectory that took them around Florida and north-ward on the Atlantic Coast of North America (Young et al., 2012). These results indicate a large difference in dispersal distance based on depth and the oceanographic currents that a migrating larva would experience. However, *T. naticoidea* adults have not yet been found outside of the Gulf of Mexico and the Caribbean. Yet, *T. naticoidea* larvae have been found to be tolerant of a wide range of temperatures (this study; Van Gaest, 2006; Arellano et al., 2014), have been found near the surface of the Gulf (Arellano et al., 2014), and have been modeled to potentially disperse throughout the Gulf and beyond in the Atlantic Ocean (Young et al., 2012), so future sampling may reveal other populations.

Larval Physiology

My work in this study measured the respiration rates of *T. naticoidea* larvae that had recently hatched, but the larval respiration rate may fluctuate due to the larvae growing and feeding during a vertical migration. A study of the Pacific oyster, *Crassostrea gigas*, evaluated

respiration in response to feeding on *Isochrysis galbana* after starvation at 23°C. Ten-day-old, unfed larvae had a respiration of approximately 3 pmol O_2 $hour^{-1}$ $larva^{-1}$ while ten-day-old larvae that were fed after two and five days of starvation had approximate respiration rates of 20 and 18 pmol O_2 $hour^{-1}$ $larva^{-1}$, respectively. Oyster larvae that were 25 days old were fed after 14 and 17 days of starvation and had approximate respiration rates of 40 and 35 pmol O_2 $hour^{-1}$ $larva^{-1}$, respectively (Moran & Manahan, 2004). The study by Moran and Manahan (2004) is especially relevant because the oysters respired at higher rates after being fed following a prolonged starvation period and shows that as Pacific oyster larvae grow and age, their respiration rate increases. Thus, *T. naticoidea* larvae might conserve or alter their respiration rate as they grow and develop during a vertical migration through a food-poor water column, which would influence the total time for their migration.

While *T. naticoidea* larvae have a high chance of survival in water temperatures above their *pejus* temperature, they may be experiencing stress due to warmer temperatures above 21°C, indicated by the plateau of their respiration rate (Figure 4) and possibly resulting in a decrease of their fitness. Arellano et al. (2014) found 11 *T. naticoidea* larvae within the upper 100 meters of the water column above the Brine Pool in the Gulf of Mexico in February 2003 when the water temperatures were approximately 17 to 20°C. Arellano et al. (2014) also evaluated the temperature tolerances of *T. naticoidea* larvae and showed 100% survival to 29 °C but significantly lower survival at 32°C, with no survival at 35 °C. This study found a possible *pejus* temperature of 21°C for *T. naticoidea* (Figure 4). The water temperature for the upper 100 meters of the water column above the Brine Pool in June 2021 was approximately 20 to 29°C (Figure 2). Based on the results from Arellano et al. (2014) and this study, *T. naticoidea* larvae can tolerate the water temperatures representing a range of seasonal surface waters in the Gulf of

Mexico. The average sea surface temperature in the Gulf varies between 23°C in April, 29.5°C in August, and 26°C in October (Müller-Karger et al., 2015). *T. naticoidea* larvae at or near the surface of the Gulf would not be exposed to lethal temperatures.

Furthermore, this study found a maximum respiration rate for *T. naticoidea* larvae at a possible *pejus* temperature of 21°C (Figure 4), and while this water temperature corresponding to a depth in the Gulf of Mexico will seasonally fluctuate, vertically migrating larvae may have some windows of time where they are achieving their optimal respiration rate. *T. naticoidea* larvae hatch from egg capsules typically from April to the late-season release through the month of September (Van Gaest 2006). The sea surface temperatures in the Gulf of Mexico have a large range across this time (Müller-Karger et al., 2015). However, early-season larvae hatching between February and April that swim vertically for 13.5 days (up to 200 m depth at a mean vertical swimming velocity of 1.43 m h^{-1}) would experience average surface water temperatures of 22 to 22.5°C, which is close to the *pejus* temperature for their respiration. Larvae hatching and swimming vertically between April and May during the mid-season would experience average surface water temperatures of 22.5 to 24.5°C, above their *pejus* temperature, and the larvae would likely begin to decrease in respiration rate (Figure 4) and possibly experience some stress. Larvae that hatch from June to mid-September would be exposed to temperatures from 27.5 to 29.5, almost 30°C (Müller-Karger et al., 2015). While the high temperatures in the late-season are not 100% lethal (Arellano et al. 2014), the larvae could be stressed near the surface. Early- and mid-season larvae that hatch between February and May would encounter the ideal temperature ranges near the surface and would be able to take advantage of the abundance of phytoplankton available without being stressed.

Swimming velocities were highly variable and there was no clear change in velocity as a function of water temperature (Figure 3), which is irregular because swimming velocity should increase in response to increasing temperature (Young, 1995). However, the variable swimming velocities of this study are similar to the results of Van Gaest (2006). Who measured a mean vertical swimming velocity of *T. naticoidea* at 8, 15, 25, and 30°C to be ($\bar{x}$ ± 1 Standard Error) 0.98 ± 0.33 mm s^{-1}, 1.61 ± 0.7 mm s^{-1}, 1.15 ± 0.28 mm s^{-1}, and 1.51 ± 0.58 mm s^{-1}, respectively, and higher than my measured mean velocities (0.42 ± 0.03 mm s^{-1}, 0.41 ± 0.03 mm s^{-1}, 0.36 ± 0.04 mm s^{-1}, 0.32 ± 0.05 mm s^{-1}, and 0.42 ± 0.04 mm s^{-1}, Figure 3). Two reasons for the difference in the range of values for vertical swimming velocity are the possibility of a phototaxis response by the larvae examined by Van Gaest (2006), and the method of measuring the swimming larvae. First, my study was performed in the dark to avoid a phototaxis response of the larvae while the velocities in Van Gaest (2006) could have been influenced by the larvae swimming faster toward the light. Second, my study used a pre-defined selection process for the vertically swimming larvae within the cuvettes but could not account for re-sampling of individual larvae. Van Gaest (2006) measured the observed swimming larvae without a selection protocol, but following observation, the larvae were removed from the cuvette to ensure that they were not re-sampled.

The variation in the larval vertical swimming velocities that I found in this study could also be attributed to the quality of the larvae that were examined. There are many factors that could contribute to larval quality. A possible reason, especially for organisms that live in a hostile environment like the deep-sea, could be phenotypic variation due to parental investment (Shima & Swearer, 2009). Differences in individual parental fitness such as feeding rate and vitellogenic mechanisms, the accumulation of yolk in a developing oocyte, play a major role in

the quality of yolk in the oocytes (Jaeckle, 1995). The individual parental differences translated through egg production directly influence the success of the offspring. For *T. naticoidea* oocytes and egg capsules, this would subsequently impact larval development. Furthermore, the larvae of *T. naticoidea* typically hatch from their egg capsules in the early spring to summer months (Van Gaest, 2006). The larvae used for the swimming experiments in my study hatched in June 2021, near the end of the expected hatching season. Late-season hatching implies a later deposition of egg capsules, potentially near the end of the reproductive season for the maternal snails when they may have depleted their mature oocytes (Van Gaest, 2006). If the larvae were less robust due to late-season deposition and maternal reproductive exhaustion, this could explain the individual larval differences of swimming performance.

Alternatively, the larvae of *T. naticoidea* might have high variability in swimming speeds, but exhibit a Type 2 acclimation response meaning there is no compensation or change in swimming rate in response to changing water temperature (Willmer et al., 2005). This ability may have allowed them to maintain a conserved vertical swimming velocity across all temperatures. In my study, every larva was exposed to all five temperature treatments, beginning at the lowest temperature of 6°C and proceeding up to 31°C in a process that took many hours, with an approximately one-hour gradual increase between target temperatures. During this hour the larvae were in the dark room, warming with the room, and were adjusting to the gradual temperature increase. The ability of the larvae to adjust to a gradual temperature increase would serve them well *in situ* during a vertical migration from the bottom of the Gulf into the surface waters, where these larvae have previously been collected (Arellano et al., 2014). An avenue for future study for these larvae, and other deep-sea larvae that undergo vertical migrations would be to evaluate the larval acclimation response to the changing temperature gradient. Also, to

elucidate whether *T. naticoidea* and other larvae exhibit capacity acclimation, changing their swimming rate due to a prolonged temperature exposure, or resistance acclimation, a change in their temperature tolerance with a conserved swimming velocity, particularly at the upper and lower temperature extremes (Willmer et al., 2005). This could be done by evaluating different physiological rates or enzymatic functions at a wide range of different temperatures.

Suggestions for future experiments

Incorporating Calorimetry

The goal of performing calorimetry was to compare the modeled cumulative expended energy of vertically swimming larvae with the actual caloric reserves that the larvae have when they hatch from the egg capsules. The initial caloric content of the larvae could indicate how far the larvae could swim and if they needed to consume food to undertake a long-distance vertical migration. When the larvae hatch, if they have more energy than what they expend during a vertical migration, they may not need to feed during their vertical migration. Conversely, if the larvae do not have the initial energy reserves required to afford the expended energy to migrate, they would need to feed on any available food resources to sustain their development. However, because combustion of an entire larval sample (*i.e.*, shell and all organic material) is the gross heat of combustion given by the calorimeter, it should to be adjusted to account for the non-organic material. Without data for caloric content of larval shells, the gross heat value of the calorimeter should approximate the caloric reserves that the larvae have when they hatch.

Two research cruises to the Gulf collected larval samples from the Brine Pool to be used in calorimetry experiments. Despite having 1,793 larvae that were collected within two days after hatching, their combined mass was only 0.0013 grams. The low mass of larvae is below the operating limit of the calorimeter (0.020 grams) and the larval sample had to be augmented with

0.0937 grams of benzoic acid to reach an acceptable mass for combustion. The one pellet of larval sample and benzoic acid resulted in a complete combustion, but the properly calibrated calorimeter recorded a negative value for the gross heat of combustion, -1,491.3 cal g^{-1}. The negative value implies that the combustion of the larvae removed heat from the system, which is not possible. A more likely scenario is that the larger benzoic acid spike made it difficult for the calorimeter to detect the small larval sample mass.

The Parr calorimetric thermometer that I used in this study is capable of correcting for an added spiking material mass to samples that are small, have a low heat of combustion, or have high water content preventing a complete combustion (Parr Instrument Company, 2010). The calculation for spiking correction is:

$$H_c = \frac{WT - e_1 - e_2 - e_3 - (H_{cs}) \cdot (m_s)}{m} \quad (5)$$

Where H_c is the heat of combustion in calories $gram^{-1}$, W is the energy equivalent value determined through calibration in calories $°C^{-1}$, T is the temperature rise in °C – the temperature change due to combustion, e_1 is the nitric acid correction factor in calories, e_2 is the sulfuric acid correction factor in calories, e_3 is the fuse correction factor in calories, H_{cs} is the heat of combustion of the spiking material – benzoic acid is 6318 calories $gram^{-1}$, m_s is the mass of the spiking material in grams, m is the mass of the sample in grams (Parr Instrument Company, 2010). Inputting the values from Table 5 into the above equation yields:

$$H_c = \frac{\left(482.745\ \frac{cal}{℃}\right) \cdot (1.274℃) - 10cal - 0cal - 15cal - \left(6318\frac{cal}{g}\right) \cdot (0.0937g)}{0.0013g} \quad (6)$$

Solve for H_c

$$H_c = -7{,}702.8\ cal\ g^{-1}$$

I chose to use the default correction factors for nitric acid and sulfuric acid, which were provided by the Parr calorimeter. I do not know what went wrong with the spiking correction calculation performed by the Parr calorimeter. However, the large negative values in the gross heat of combustion, combined with the discrepancies in the values between the manual calculation in equation 6 and the value provided in Table 5, indicates to me that more larval sample is required. In addition, while the calorimeter was properly calibrated (Appendix Table A), the large difference between the spike and the larval sample meant that any possible signal that the calorimeter could have measured for the combustion of the larvae would have been muddled by the combustion of the benzoic acid. This could have been avoided by using a smaller mass of benzoic acid spiking material, while still using enough spiking material to reach the suitable mass range for combustion and detection by the calorimeter. There may also be additional reasons for the negative value, -1,491.3 calories g^{-1}, given by the calorimeter in Table 5.

The initial temperature of the jacket was higher (approximately 20°C, Table 5) than the mean jacket temperature for the calibration runs (approximately 17°C, Appendix Table 1). The high jacket temperature for the combustion of the pellet with larvae and benzoic acid was due to

the time it took to make the pellet. I filled the jacket with water, identically to the calibration procedure, and then spent time tamping, forming, and massing the pellet of benzoic acid and larvae. During this time, the water was sitting in the jacket, warming with the ambient laboratory temperature and the residual heat of the calorimeter. The increase in the jacket temperature could have skewed the calculations performed by the calorimeter because the energy equivalent value incorporates a specific initial jacket temperature and temperature rise due to combustion, which was different for the combustion of the pellet. The combination of the higher than usual jacket temperature and the large amount of spiking material ultimately are what could have resulted in the negative value for combustion of the larval sample. When performing bomb calorimetry, it is imperative that sample preparation methods be exact, precise, and identical to calibration preparation methods.

As an alternative method to calorimetry, proximate biochemical analyses can be considered to determine the protein and lipid content of the larvae. In bivalve and gastropod veligers, the lipid, fatty acid, and protein content of food resources like algae correlates to faster development and increased survival of larvae (Boidron-Métairon, 1995). Utilizing proximate biochemical analyses could indicate the average lipid and protein content of the larvae (Craig et al., 1978), which can then be used to calculate the calories contained within those lipids, fatty acids, and proteins. However, these analyses also require a large number of larvae for analysis so this method would not have been feasible in this project.

An Improved Migration Model

The migration model from Young et al. (1996), used in this study, does not account for changes in water viscosity due to changing temperature. As the larvae migrate vertically from deep cold water to relatively warm surface water, the change in water viscosity would influence

the larval swimming speed (Podolsky & Emlet, 1993). As viscosity decreases near the warmer surface water, the larvae are likely to accelerate, meaning the larvae would reach the surface sooner. The change in the velocity can be accounted for in the migration model by altering the constant velocity component into a velocity function.

The migration model in equation 7 should be used if the water temperature is found to influence the larval vertical swimming velocity because this model utilizes a Q_{10} value for two velocities at two water temperatures corresponding to specific depths. This improved migration model now accounts for the change in velocity due to water temperature and water depth during a vertical migration by a swimming larva. It also includes changes in water viscosity, to the extent that changing viscosity influences the swimming velocity. Additionally, equation 7 can be generalized to cases where the water temperature or velocity are not a linear function of water depth because of the non-linear relationship in equation 8. The equations and derivations for the following modified migration model are in Appendix B (section *Derivation of augmented migration model that includes temperature dependent swimming velocity*).

$$E_t = \int_{t_0}^{t} K Q_0 e^{-r_1 mat \frac{1}{(e^{-bh_0} - abt)}} \, dt \tag{7}$$

$$a = v_0 e^{-r_2 m h_0} \tag{8}$$

$$b = r_2 m \tag{9}$$

$$r_2 = 0.1℃ \cdot \ln(Q_{10}) \tag{10}$$

In this equation, the output E_t, is the cumulative expended energy in Joules. Input variables include: K is a conversion factor for energy units (*i.e.*, oxyenthalpic equivalent Gnaiger, 1983); Q_0 is the initial rate of metabolism at t_0 in pmol O_2^{-1} hour^{-1} larva^{-1}; r_1 is the rate of change of metabolism as a function of temperature in pmol O_2^{-1} hour^{-1} larva^{-1} °C^{-1}; m is the rate of change of the temperature of the water column as a function of depth in °C meter^{-1}; a represents the change in swimming velocity due to water temperature; v_0 is the swimming velocity at t_0; r_2 incorporates the Q_{10} value of the ratio of swimming velocities for a desired vertical distance bin and in units of °C; m is the rate of change of the water temperature as a function of depth; h_0 is the water depth at t_0; b is the combination of r_2 and m; and t is time. This new, more complex vertical migration model could be evaluated at discrete intervals corresponding to vertical distance bins for a desired resolution.

Jaeckle and Manahan (1992) found that the dissolved organic matter components of seawater play a major role in the alteration of respiration rates of larvae from a gastropod and an urchin. Additionally, Moran and Manahan (2004) found pacific oyster larvae that have been starved have higher respiration rates after being fed algae. These two studies have huge implications for the migration model derived in this study, and the model from Young et al. (1996). The models only account for the change in respiration rate due to changing temperature and do not account for the change in respiration rate due to the organic components of the

seawater or the presence of food. It is possible the food-related factors that influence the respiration rate could be combined into the migration model. Attempting to incorporate all relevant pieces of information into one migration model will further elucidate the expended energy of a vertically swimming larva.

Conclusion

This study examined how the vertical swimming velocities and respiration of *T. naticoidea* larvae were influenced by water temperature and used the migration model from Young et al. (1996) to elucidate how much energy a *T. naticoidea* larva might expend during a vertical migration to provide context for their available food resources. The migration model revealed that the larvae might expend 52.7 mJ to reach the photic zone at 200 meters depth. However, we still need empirical values of initial larval energy reserves to know whether the stored energy exceeds the expended energy. Additionally, this study built upon the model from Young et al. (1996), deriving a migration model that can account for changes in vertical swimming velocity of a larva during a vertical migration that can more accurately estimate migration potential.

As the larvae vertically migrate from 650 meters up to the surface, they have access to food like dissolved organic materials and bacteria. Although, whether the larvae can assimilate dissolved organic materials without eating remains to be verified. Once at the surface, depending on the time of year, they have access to phytoplankton which they can eat to continue their development. Migration through a 650-meter water column will expose larvae to a dynamic current system that can ultimately impact their dispersal and population connectivity (Young et al., 2012; McVeigh et al., 2017). In the future, vertical migration models, like the one derived in

this study or from Young et al. (1996), can be incorporated with larval transport models to predict larval dispersal distances and population connectivity more accurately.

Works Cited

Anger, K., & Dawirs, R. (1981). Influence of starvation on the larval development of Hyas araneus (Decapoda, Majidae). *Helgoländer Meeresuntersuchungen*, *34*, 287–311.

Arellano, S. M. (2008). *Embryology, Larval Ecology, and Recruitment of "Bathymodiolus" Childressi, a Cold-Seep Mussel from the Gulf of Mexico* [Dissertation]. University of Oregon.

Arellano, S. M., Van Gaest, A. L., Johnson, S. B., Vrijenhoek, R. C., & Young, C. M. (2014). Larvae from deep-sea methane seeps disperse in surface waters. *Proceedings of the Royal Society B: Biological Sciences*, *281*(1786), 20133276. https://doi.org/10.1098/rspb.2013.3276

Arellano, S. M., & Young, C. M. (2011). Temperature and salinity tolerances of embryos and larvae of the deep-sea mytilid mussel "Bathymodiolus" childressi. *Marine Biology*, *158*(11), 2481–2493. https://doi.org/10.1007/s00227-011-1749-9

Boidron-Métarion, I. F. (1995). Larval Nutrition. In L. McEdward (Ed.), *Ecology of Marine Invertebrate Larvae* (pp. 223–248). CRC Press.

Bouchet, P., & Warén, A. (1994). Ontogenetic Mirgration and Dispersal of Deep-Sea Gastropod Larvae. In *Reproduction, Larval Biology, and Recruitment of the Deep-Sea Benthos* (pp. 98–117). Columbia University Press.

Cartes, J. E. (1998). Dynamics of the bathyal Benthic Boundary Layer in the northwestern Mediterranean: Depth and temporal variations in macrofaunal-megafaunal communities and their possible connections within deep-sea trophic webs. *Progress in Oceanography*, *41*, 111–139.

Clarke, A. (1989). New mollusks from undersea oil seep sites off Louisiana. *Malacology Data Net*, *2*(5/6), 122–134.

Craig, J. F., Kenley, M. J., & Talling, J. F. (1978). Comparitive estimations of the energy content of fish tissue from bomb calorimetry, wet oxidation, and proximate analysis. *Freshwater Biology*, *8*(6), 585–590.

Fiksen, Ø., Jørgensen, C., Kristiansen, T., Vikebø, F., & Huse, G. (2007). Linking behavioural ecology and oceanography: Larval behaviour determines growth, mortality and dispersal. *Marine Ecology Progress Series*, *347*, 195–205. https://doi.org/10.3354/meps06978

Flögel, S., & Dullo, W.-C. (2011). High-resolution water mass measurements around cold-water corals: A comparative test study between repeated Conductivity-Temperature-Depth (CTD) casts and continuous data acquisition of bottom waters from the West Florida Slope, Gulf of Mexico. *Annalen Des Naturhistorischen Museums in Wien. Serie A Für Mineralogie Und Petrographie, Geologie Und Paläontologie, Anthropologie Und Prähistorie*, *113*, 209–224.

Gary, S. F., Fox, A. D., Biastoch, A., Roberts, J. M., & Cunningham, S. A. (2020). Larval behaviour, dispersal and population connectivity in the deep sea. *Scientific Reports*, *10*(1), 10675. https://doi.org/10.1038/s41598-020-67503-7

Gili, J.-M., Vendrell-Simón, B., Arntz, W., Sabater, F., & Ros, J. (2020). The benthos: The ocean's last boundary? *Scientia Marina*, *84*(4), 463–475. https://doi.org/10.3989/scimar.05091.24A

Gnaiger, E. (1983). Calculation of energetic and biochemical equivalents of respiratory oxygen consumption. *Polarographic Oxygen Sensors: Aquatic and Physiological Applications*, 337–345.

Hall, C. A., & Leben, R. R. (2016). Observational evidence of seasonality in the timing of loop current eddy separation. *Dynamics of Atmospheres and Oceans*, *76*, 240–267.

Ikeda, T., Torres, J. J., Hernández-León, S., & Geiger, S. P. (2000). 10—Metabolism. In R. Harris, P. Wiebe, J. Lenz, H. R. Skjoldal, & M. Huntley (Eds.), *ICES Zooplankton Methodology Manual* (pp. 455–532). Academic Press. https://doi.org/10.1016/B978-012327645-2/50011-6

Jaeckle, W. B. (1995). Variation in the Size, Energy Content, and Biochemical Composition of Invertebrate Eggs: Correlates to the Mode of Larval Development. In L. McEdward (Ed.), *Ecology of Marine Invertebrate Larvae* (pp. 49–77). CRC Press.

Jaeckle, W. B., & Manahan, D. T. (1989). Growth and energy imbalance during the development of a lecithotrophic molluscan larva (Haliotis rufescens). *The Biological Bulletin*, *177*(2), 237–246.

Jaeckle, W. B., & Manahan, D. T. (1992). Experimental manipulations of the organic compositions of seawater: Implications for studies of energy budgets in marine invertebrate larvae. *Journal of Experimental Marine Biology and Ecology*, *156*(2), 273–284.

Killingley, J. S., & Rex, M. A. (1985). Mode of larval development in some deep-sea gastropods indicated by oxygen-18 values of their carbonate shells. *Deep-Sea Research*, *32*(7), 809–818.

Lawlor, J. (2020). *jakelawlor/PNWColors: Initial Release* (0.1.0) [R]. Zenodo. https://doi.org/10.5281/ZENODO.3971033

McVeigh, D. M., Eggleston, D. B., Todd, A. C., Young, C. M., & He, R. (2017). The influence of larval migration and dispersal depth on potential larval trajectories of a deep-sea bivalve. *Deep Sea Research Part I: Oceanographic Research Papers*, *127*, 57–64. https://doi.org/10.1016/j.dsr.2017.08.002

Miller, N. A., & Stillman, J. H. (2012). Physiological Optima and Critial Limits. *Nature Education Knowledge*, *3*(10). https://www.nature.com/scitable/knowledge/library/physiological-optima-and-critical-limits-45749376/

Moran, A. L., & Manahan, D. T. (2003). Energy metabolism during larval development of green and white abalone, Haliotis fulgens and H. sorenseni. *The Biological Bulletin*, *204*(3), 270–277.

Moran, A., & Manahan, D. (2004). Physiological recovery from prolonged 'starvation'in larvae of the Pacific oyster Crassostrea gigas. *Journal of Experimental Marine Biology and Ecology*, *306*(1), 17–36.

Müller-Karger, F. E., Smith, J. P., Werner, S., Chen, R., Roffer, M., Liu, Y., Muhling, B., Lindo-Atichati, D., Lamkin, J., Cerdeira-Estrada, S., & others. (2015). Natural variability of surface oceanographic conditions in the offshore Gulf of Mexico. *Progress in Oceanography*, *134*, 54–76.

Müller-Karger, F. E., Walsh, J. J., Evans, R. H., & Meyers, M. B. (1991). On the seasonal phytoplankton concentration and sea surface temperature cycles of the Gulf of Mexico as determined by satellites. *Journal of Geophysical Research: Oceans*, *96*(C7), 12645–12665.

National Oceanic and Atmospheric Administration (NOAA). (2023). *What is a current?* https://oceanservice.noaa.gov/facts/current.html

Nielsen, C. (2018). Origin and Diversity of Marine Larvae. In T. J. Carrier, A. M. Reitzel, & A. Heyland (Eds.), *Evolutionary Ecology of Marine Invertebrate Larvae* (pp. 3–15). Oxford University Press. https://doi.org/10.1093/oso/9780198786962.003.0001

Parr Instrument Company. (2010). *Calculations; Corrections—Parr 6772 Calorimetric Thermometer Instruction Manual*. Manualslib. https://www.manualslib.com/manual/1542262/Parr-Instrument-6772.html?page=48#manual

Peck, L., & Prothero-Thomas, E. (2002). Temperature effects on the metabolism of larvae of the Antarctic starfish Odontaster validus, using a novel micro-respirometry method. *Marine Biology*, *141*, 271–276.

Peck, L. S., Clarke, A., & Chapman, A. L. (2006). Metabolism and development of pelagic larvae of Antarctic gastropods with mixed reproductive strategies. *Marine Ecology Progress Series*, *318*, 213–220.

Podolsky, R. D., & Emlet, R. B. (1993). Separating the effects of temperature and viscosity on swimming and water movement by sand dollar larvae (Dendraster excentricus). *The Journal of Experimental Biology*, *176*(1), 207–222.

random.org—True Random Number Service. (1998). https://www.random.org/

Selph, K. E., Swalethorp, R., R Stukel, M., B Kelly, T., N Knapp, A., Fleming, K., Hernandez, T., & R Landry, M. (2021). Phytoplankton community composition and biomass in the oligotrophic Gulf of Mexico. *Journal of Plankton Research*, *44*(5), 618–637. https://doi.org/10.1093/plankt/fbab006

Shanmugam, G. (2012). Chapter 4 Bottom-Current Reworked Sands. *Handbook of Petroleum Exploration and Production*, *9*, 129–219. https://doi.org/10.1016/b978-0-444-56335-4.00004-7

Shima, J. S., & Swearer, S. E. (2009). Larval quality is shaped by matrix effects: Implications for connectivity in a marine metapopulation. *Ecology*, *90*(5), 1255–1267. https://doi.org/10.1890/08-0029.1

Smith, C., Deleo, F., Bernardino, A., Sweetman, A., & Arbizu, P. (2008). Abyssal food limitation, ecosystem structure and climate change. *Trends in Ecology & Evolution*, *23*(9), 518–528. https://doi.org/10.1016/j.tree.2008.05.002

Staats, P., Wargula, A., & McGann, B. (2009). *Find_Larvae_Tracks_2011_bp* (07.18.11) [MatLab].

Strathmann, M. F. (1987). *Reproduction and development of marine invertebrates of the northern Pacific coast: Data and methods for the study of eggs, embryos, and larvae*. University of Washington Press.

Teixeira, S., Olu, K., Decker, C., Cunha, R. L., Fuchs, S., Hourdez, S., Serrao, E. A., & Arnaud-Haond, S. (2013). High connectivity across the fragmented chemosynthetic ecosystems of the deep Atlantic Equatorial Belt: Efficient dispersal mechanisms or questionable endemism? In *MOLECULAR ECOLOGY* (Vol. 22, Issue 18, pp. 4663–4680). WILEY. https://doi.org/10.1111/mec.12419

Van Gaest, A. L. (2006). *Ecology and early life history of Bathynerita naticoidea: Evidence for long-distnce larval dispersal of a cold seep gastropod* [Master's Thesis]. University of Oregon.

Walker, N. D., Leben, R. R., & Balasubramanian, S. (2005). Hurricane-forced upwelling and chlorophyll a enhancement within cold-core cyclones in the Gulf of Mexico. *Geophysical Research Letters*, *32*(18).

Wendt, D. E. (2000). Energetics of larval swimming and metamorphosis in four species of Bugula (Bryozoa). *The Biological Bulletin*, *198*(3), 346–356.

Wheeler, J. D., Helfrich, K. R., Anderson, E. J., McGann, B., Staats, P., Wargula, A. E., Wilt, K., & Mullineaux, L. S. (2013). Upward swimming of competent oyster larvae Crassostrea virginica persists in highly turbulent flow as detected by PIV flow subtraction. In *MARINE ECOLOGY PROGRESS SERIES* (Vol. 488, pp. 171–185). INTER-RESEARCH. https://doi.org/10.3354/meps10382

Willmer, P., Stone, G., & Johnston, I. (2005). Temperature and its Effects. In *Environmental Physiology of Animals* (Second, pp. 175–222). Blackwell Publishing.

Young, C. M. (1994). A Tale of Two Dogmas: The Early History of Deep-Sea Reproductive Biology. In C. M. Young & K. J. Eckelbarger (Eds.), *Reproduction, Larval Biology, and Recruitment of the Deep-Sea Benthos* (pp. 1–25). Columbia University Press.

Young, C. M., Arellano, S. M., Hamel, J.-F., & Mercier, A. (2018). Ecology and Evolution of Larval Dispersal in the Deep Sea. In T. J. Carrier, A. M. Reitzel, & A. Heyland (Eds.), *Evolutionary Ecology of Marine Invertebrate Larvae* (pp. 229–250). Oxford University Press. https://doi.org/10.1093/oso/9780198786962.003.0016

Young, C. M., Devin, M. G., Jaeckle, W. B., Ekaratne, S. U., & George, S. B. (1996). The potential for ontogenetic vertical migration by larvae of bathyal echinoderms. *Oceanologica Acta*, *19*(3–4), 263–271.

Young, C. M., He, R., Emlet, R. B., Li, Y., Qian, H., Arellano, S. M., Van Gaest, A., Bennett, K. C., Wolf, M., Smart, T. I., & Rice, M. E. (2012). Dispersal of Deep-Sea Larvae from the Intra-American Seas: Simulations of Trajectories using Ocean Models. *Integrative and Comparative Biology*, *52*(4), 483–496. https://doi.org/10.1093/icb/ics090

Zande, J. M., & Carney, R. S. (2001). Population Size Structure and Feeding Biology of Bathynerita naticoidea Clarke 1989 (Gastropoda: Neritacea) from Gulf of Mexico Hydrocarbon Seeps. *Gulf of Mexico Science*, *19*(2). https://doi.org/10.18785/goms.1902.04

Zigler, K. S., Lessios, H. A., & Raff, R. A. (2008). Egg energetics, fertilization kinetics, and population structure in echinoids with facultatively feeding larvae. *The Biological Bulletin*, *215*(2), 191–199.

Appendix A

Figures and Tables

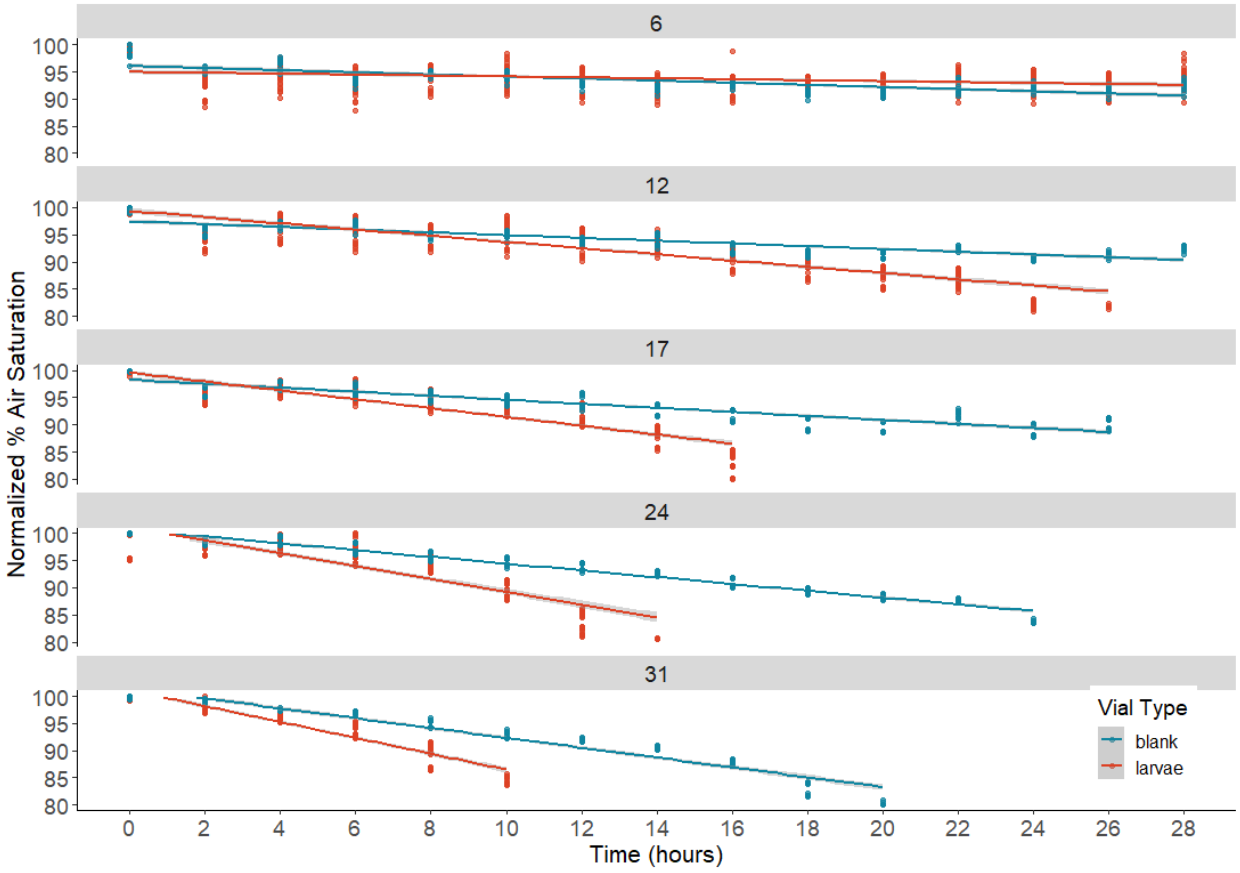

Appendix Figure A – Respiration of larvae in vials across time and within the temperature treatments of 6, 12, 17, 24, and 31°C. Data points represent replicate measurements for both the replicate blank and larvae vials. Air saturation was normalized to be on a 100% scale because air saturation can be over 100% in sea water. The respiration rates of the blank vials are less than 5% of the respiration within the vials with larvae, except for the 6°C treatment. Colors are from PNWColors package (Lawlor, 2020).

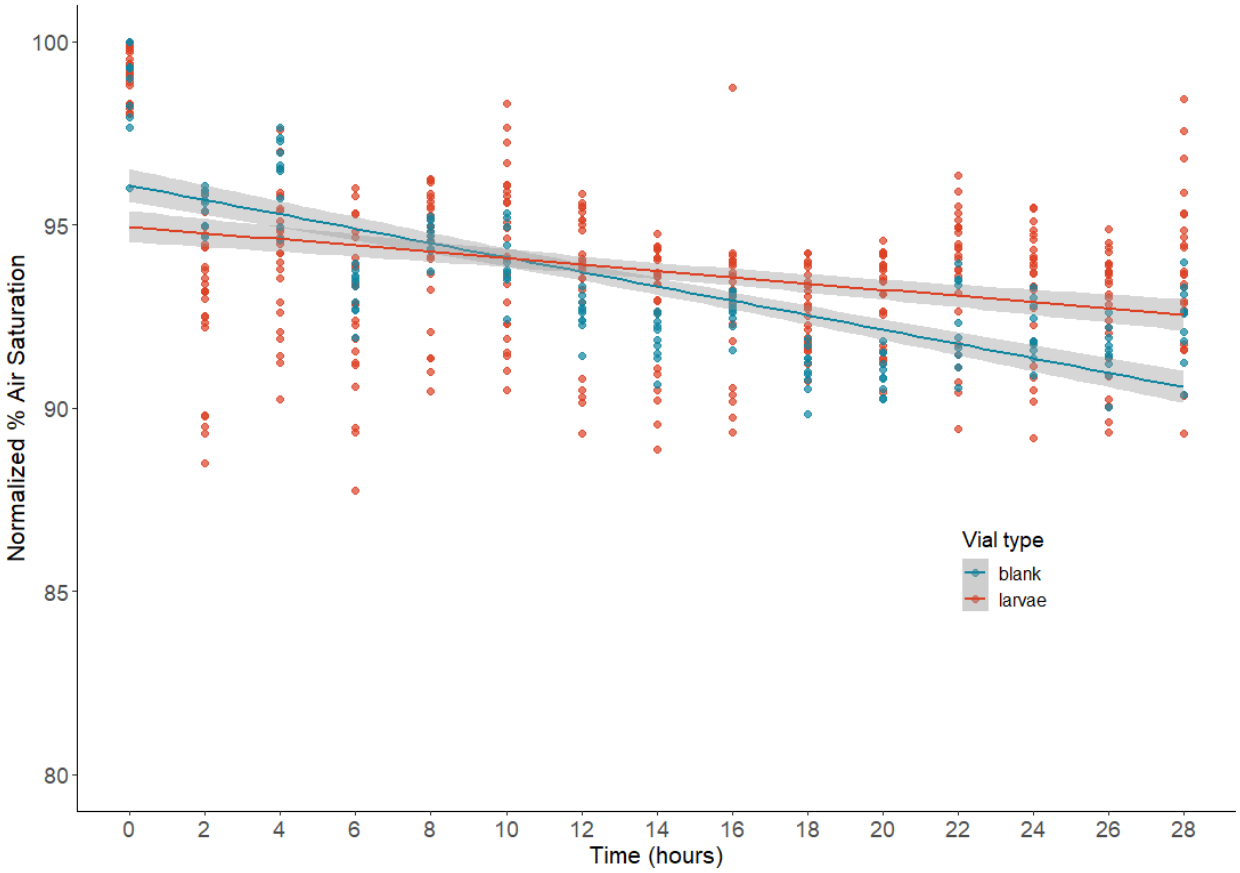

Appendix Figure B – Close up of the 6°C treatment for the respiration experiment. Data points are replicate measurements within the replicate vials for both blank vials and larvae vials. Shaded region around the lines are the 95% confidence intervals. The blank vials have a higher respiration rate than the vials with larvae (greater than 5%). Colors are from the PNWColors package (Lawlor, 2020).

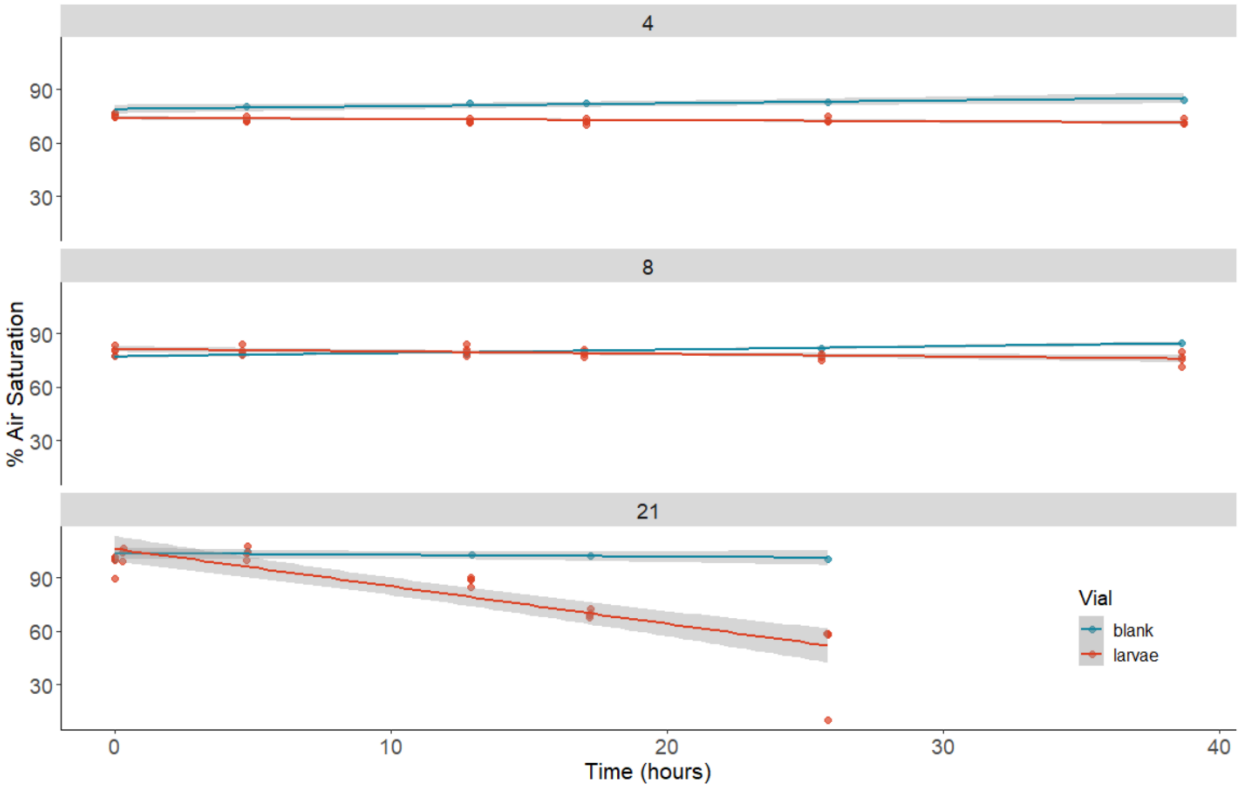

Appendix Figure C – *Thalassonerita naticoidea* respiration rate data from 2014 measured by Arellano at 4, 8, and 21°C. Data points represent replicate measurements for both the replicate blank and larvae vials. Shaded regions around the line represent the 95% confidence interval. The respiration rates of the blank vials are less than 5% of the respiration within the vials with larvae. Colors are from PNWColors package (Lawlor, 2020).

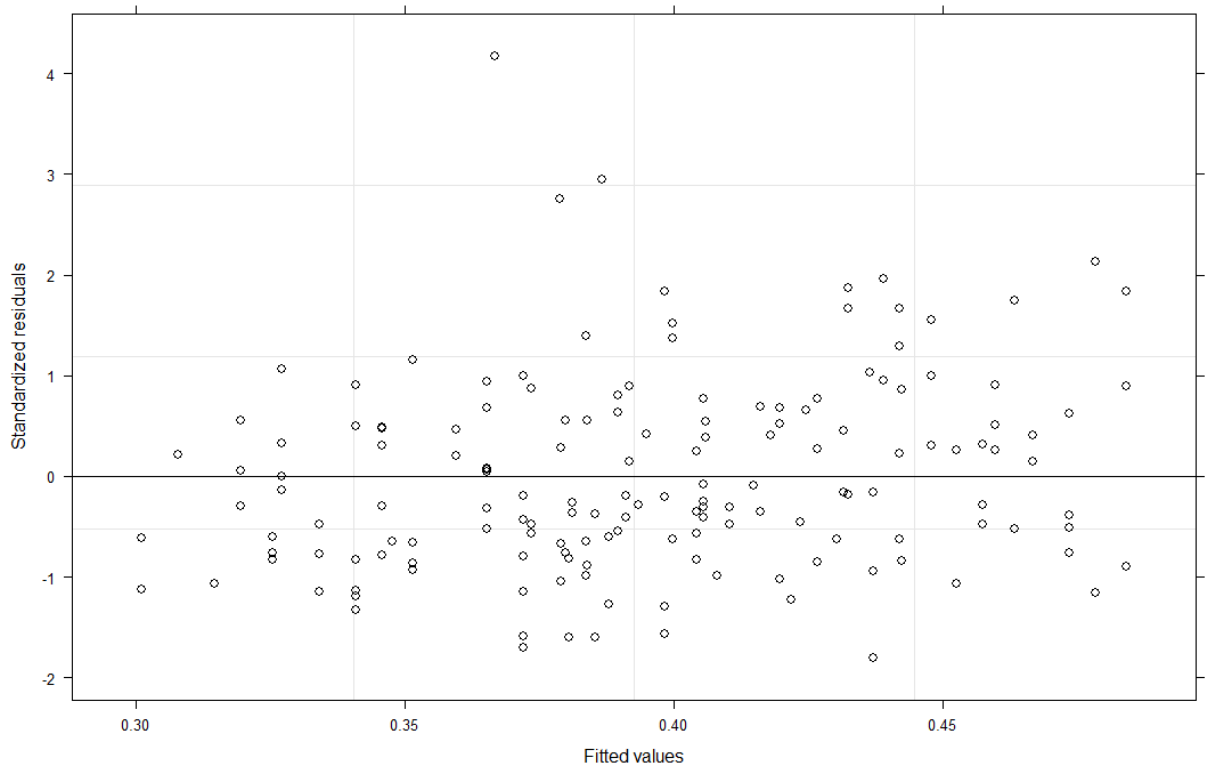

Appendix Figure D – Residuals from the parsimonious model for the swimming experiment. A linear mixed model with fixed factors of temperature, and random effects of random intercepts for the replicate cuvettes nested within temperature.

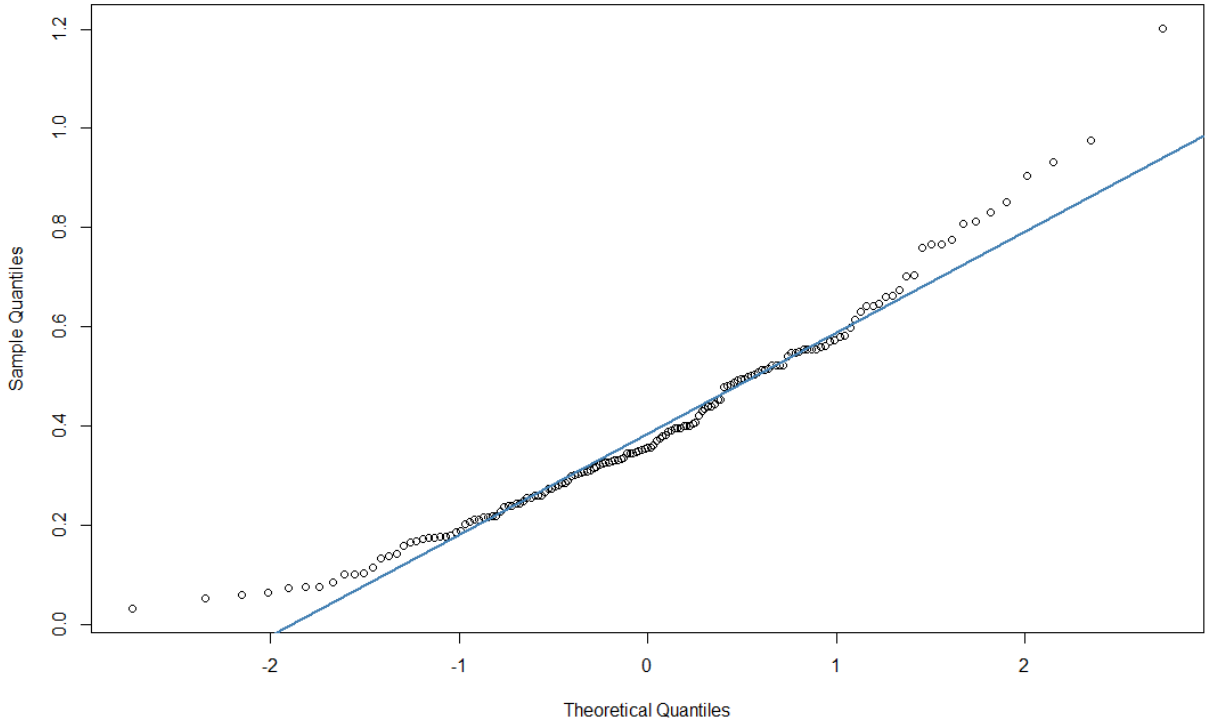

Appendix Figure E – Quantile-Quantile plot for the parsimonious model for the swimming experiment. A linear mixed model with fixed factors of temperature, and random effects of random intercepts for the replicate cuvettes nested within temperature.

Appendix Table A – Calorimeter combustion calibration runs. The heat of combustion of the benzoic acid standard used was 6318 cal g^{-1}. The relative standard deviation among the calibration runs is 0.1383%. The fuse value is the number of calories that are consumed by the combusted wire. The acid value is the number of calories extracted from the bomb system due to formation of nitric acid via combustion. The Energy Equivalent (EE) value is calculated by the Parr thermometer.

Sample ID	Initial Temp (°C)	Jacket Temp (°C)	Temp rise (°C)	Sample mass (g)	Fuse (cal)	Acid (cal)	EE value (cal $°C^{-1}$)	Gross Heat (cal g^{-1})
24	17.8309	19.4188	2.6246	0.19630	15.0000	10.0000	482.091	6329.48
19	16.9098	18.4023	2.6135	0.19570	15.0000	10.0000	482.691	6320.39
18	17.2002	19.8657	2.5887	0.19430	15.0000	10.0000	483.896	6304.56
17	17.0679	19.5952	2.5776	0.19320	15.0000	10.0000	483.281	6311.01
16	16.8377	19.7512	2.6388	0.19760	15.0000	10.0000	482.614	6318.86
15	16.8915	19.7812	2.7486	0.20580	15.0000	10.0000	482.173	6324.83
14	17.0049	19.8182	2.6291	0.19660	15.0000	10.0000	481.988	6328.59
13	17.1080	19.9738	2.5818	0.19360	15.0000	10.0000	483.480	6311.21
12	17.0984	19.7639	2.6277	0.19670	15.0000	10.0000	482.487	6322.07

Appendix Table B – Model selection for swimming experiment data. The most parsimonious model indicated by (*) was chosen for the swimming experiment. Linear mixed models were compared to the generalized least squares model by evaluating the Akaike Information Criterion scores.

Model	AIC
Generalized Least Squares	
Velocity ~ Temperature	-25.3
Linear Mixed Models	
Fixed Effect	
Velocity ~ Temperature	
Random Effects	
Random intercepts for replicate cuvettes nested in temperature *	-27.4
Random intercepts for replicate cuvettes and random slopes across temp.	-25.1

Appendix B

Derivation of augmented migration model that includes temperature dependent swimming velocity

The work of Young et al. (1996) developed a numerical model for the cumulative expended energy of a vertically swimming larva, and this allows us to set bounds on the possible extent of their migration. The model suggested that long distance vertical migrations are more influenced by physiological tolerances than by the energy reserves of a larva. One assumption of the model is the swimming velocity is independent of the water temperature. However, Podolsky and Emlet (1993) demonstrated that water temperature and viscosity can greatly impact the swimming velocity of larvae.

The purpose of this annex section is to propose an extension of the Young et al. (1996) cumulative expended energy model that incudes temperature dependent vertical swimming velocity. We first rederive the Young et al. (1996) model in detail and then build on that work.

Relevant rate equations

Beginning with the standard Arrhenius form for a rate:

$$rate = Ae^{\left(-\frac{E_a}{KT}\right)} \tag{1}$$

Where A is a constant, E_a is the activation energy, K is boltzman's constant, and T is absolute temperature in Kelvin.

A common concept in energy is the ratio of two rates, *r*, which can be defined as:

$$\frac{rate_2}{rate_1} = e^{r\Delta T} \tag{2}$$

with

$$r = \frac{E_a}{KT_2 - T_1} \tag{3}$$

$$\Delta T = T_2 - T_1 \tag{4}$$

and T_2 and T_1 are the absolute temperatures in Kelvin at $rate_2$ and $rate_1$, respectively.

The above rate ratio is similar to the concept of Q_{10} where the change in the rate is specified to a 10°C change in temperature:

$$Q_{10} \equiv \left(\frac{rate_2}{rate_1}\right)^{\frac{10°C}{\Delta T}} \tag{5}$$

$$Q_{10} = e^{r\Delta T \cdot \frac{10°C}{\Delta T}} \tag{6}$$

$$Q_{10} = e^{r \cdot 10°C} \tag{7}$$

$$\therefore r = \frac{ln(Q_{10})}{10℃}$$

(8)

Assuming that larval vertical swimming velocity is a function of depth and the surrounding water temperature, through experimentation, it is possible to calculate a Q_{10} value that describes the change in vertical swimming velocity due the water temperature.

$$v = v_0 e^{r_2 \Delta T}$$

(9)

$$r_2 = 0.1℃ \cdot ln(Q_{10})$$

(10)

Where v is the vertical swimming velocity after swimming through the water depth and temperature bounded at T_2 and T_1, and r_2 incorporates the Q_{10} value for the ratio of the swimming velocities within this bound.

Deriving the temperature and depth relationships

We now define a coordinate system. For this derivation, swimming velocity is positive if directed toward the surface. Depth is a negative number, where the surface is $h = 0$. Note that this coordinate definition is different than Young et al. (1996) in that depth is defined as a negative number, *i.e.*, below the surface. Also, from Young et al. (1996), we assume a linear relationship between water temperature and water depth:

$$T(h) = mh + b$$

(11)

Where *m* is the slope, the rate of change of the water temperature as a function of the water depth, *h*, and *b* is the y-intercept.

$$\therefore\ \Delta T = mh_1 - mh_0$$

(12)

Where h_0 is the starting water depth at T_0 and h_1 is the water depth at T_1. Assuming the larvae swim at a constant effective rate of *v*, $h_1 = vt$, where *t* is the time to swim from h_0 to h_1.

Simplifying

$$\Delta T = mvt$$

(13)

Total energy formula assuming a constant swimming velocity

Substituting equation 13 into equation 2 and converting energy from moles O_2 to mJ using the conversion factor of 480 mJ µmol O_2^{-1}, yields equation 14 from Young et al. (1996) for the cumulative expended energy of a vertically swimming larva as a function of time.

$$E(t) = KQ_0e^{rmvt}$$

(14)

The total expended energy is:

$$E_{total} = \int_{t_0}^{t_1} KQ_0 e^{rmvt} dt = \left(\frac{KQ_0}{rmv}\right) e^{rmvt_1} - \left(\frac{KQ_0}{rmv}\right) e^{rmvt_0}$$

(15)

Note the sign of this derivation is opposite that of Young et al. (1996) because we defined depth to be a negative number with the surface at $h = 0$, and the starting depth, h_0, is the starting depth multiplied by -1.

Energy calculation with a temperature or depth dependent swimming velocity

In the following, the vertical swimming velocity is not assumed to be constant, but rather a function of time, water depth, or water temperature. Thus, we seek to derive a function for vertical swimming velocity as a function of time to substitute into the derivation of equation 15.

The vertical velocity as a function of larva position in the water column can be viewed as:

$$v(h) = v_0 e^{r_2 m h_1 - r_2 m h_0}$$

(16)

where v_0 is the velocity at the starting depth of h_0 at temperature T_0, r_2 is the rate of change of velocity with temperature given by equation 10, and m is the change in water temperature with depth. Simplifying:

$$v(h) = v_0 e^{-r_2 m h_0} e^{r_2 m h_1}$$

(17)

And making a variable substitution to simplify the math:

$$a = v_0 e^{-r_2 m h_0} \tag{18}$$

$$b = r_2 m \tag{19}$$

$$v(h) = a e^{b h_1} \tag{20}$$

Water depth, h_1, is dependent on the larva actively swimming from the starting position of h_0 and will be replaced with x.

$$v(x) = a e^{bx} \tag{21}$$

Equation 21 provides the velocity as a function of position. Assuming the swimming larva only travels in one dimension and velocity is never zero, the velocity and position as functions of time are related by:

$$v\big(x(t)\big) = \frac{dx(t)}{dt} \tag{22}$$

Rearranging to express as a differential equation:

$$dt = \frac{dx(t)}{v(x)}$$

(23)

Substituting equation 21 into equation 23 and solving the differential equation for *t* yields:

$$\int dt = \int \frac{1}{a} e^{-bx} dx$$

(24)

$$t = \int_{x(0)}^{x(t)} \frac{1}{a} e^{-bx} dx$$

(25)

$$t = \frac{-1}{ab} e^{-bx} + c \,|_{x(0)}^{x(t)}$$

(26)

The integration constant, *c*, is determined by using the boundary condition: at $t = 0$, $x(0) = h_0$. The solution for *t* as a function of position is:

$$t = \frac{-1}{ab}\left(e^{-bx(t)} - e^{-bx(0)}\right)$$

(27)

Rearranging to solve for $x(t)$.

$$x(t) = \frac{-1}{b} ln(e^{-bh_0} - abt)$$

(28)

We can now check to ensure the solution is valid at the boundary condition: at $t = 0$, $x(0) = h_0$.

$$x(0) = h_0 = \frac{-1}{b} ln(e^{-bh_0} - 0)$$

(29)

$$h_0 = h_0$$

(30)

The boundary condition is satisfied.

Now that we have the position function $x(t)$, we take the derivative to get the velocity function $v(t)$.

$$v(t) = \frac{d\,x(t)}{dt} = \frac{-1}{b} \cdot \frac{-ab}{e^{-bh_0} - abt}$$

(31)

Simplify.

$$v(t) = \frac{a}{e^{-bh_0} - abt}$$

(32)

where

$$a = v_0 e^{-r_2 m h_0}$$

(33)

$$b = r_2 m$$

(34)

$$r_2 = 0.1℃ \cdot ln(Q_{10})$$

(35)

The time dependent vertical swimming velocity from equation 32 can be substituted into the original model by Young et al. (1996), equation 15.

$$E_t = \int_{t_0}^{t} K Q_0 e^{-r_1 mat \frac{1}{(e^{-bh_0} - abt)}} dt$$

(36)

$$a = v_0 e^{-r_2 m h_0}$$

(37)

$$b = r_2 m$$

(38)

$$r_2 = 0.1 \cdot \ln(Q_{10})$$

(39)

Unlike the solution provided by Young et al. (1996), the integral in equation 36 does not appear to have a closed solution and must numerically integrated. This improved migration model now accounts for the change in velocity due to water temperature and water depth during a vertical migration by a swimming larva. It also includes changes in water viscosity to the extent that those changes influence the swimming velocity. Furthermore, this derivation can be generalized to cases where the water temperature or velocity are not a linear function of water depth.